8 Boltzmann Transport in Condensed Matter

Franz Xaver Bronold

Institut für Physik, Universität Greifswald, 17487 Greifswald, Germany

This chapter presents numerical methods for the solution of Boltzmann equations as applied to the analysis of transport and relaxation phenomena in condensed matter systems.

8.1 Boltzmann Equation for Quasiparticles

Besides the traditional approaches, such as variational methods or the expansion of the distribution function in a symmetry adapted orthonormal set of functions, stochastic methods, either based on the sampling of the distribution function by superparticles, the particle-in-cell Monte Carlo collision (PIC-MCC) approach, or the direct simulation of the master equation underlying the Boltzmann description, the ensemble Monte Carlo methods, are discussed at a tutorial level. Expansion methods are most appropriate for the solution of Boltzmann equations which occur in the Fermi liquid based description of transport in normal metals and superconductors. Stochastic methods, on the other hand, are particularly useful for the solution of relaxation and transport problems in semiconductors and electronic devices.

8.1.1 Preliminary Remarks

The Boltzmann equation (BE) is of central importance for the description of transport processes in many-particle systems. Boltzmann introduced this equation in the second half of the 19^{th} century to study irreversibility in gases from a statistical mechanics point of view. Envisaging the molecules of the gas to perform free flights, which are occasionally interrupted by mutual collisions, he obtained the well-known equation [1]

$$\frac{\partial g}{\partial t} + \boldsymbol{v}\cdot\nabla_{\boldsymbol{r}} g + \frac{\boldsymbol{F}}{M}\cdot\nabla_{\boldsymbol{v}} g = \left(\frac{\partial g}{\partial t}\right)_c , \tag{8.1}$$

where $g(\boldsymbol{r},\boldsymbol{v},t)$ is the velocity distribution function, M is the mass of the gas molecules, $\boldsymbol{F}$ is the external force, and the r.h.s. is the collision integral. With this equation Boltzmann could not only prove his famous H-theorem, which contains a definition of entropy in terms of the velocity distribution function and states that

F. X. Bronold: *Boltzmann Transport in Condensed Matter*, Lect. Notes Phys. **739**, 223–254 (2008)
DOI 10.1007/978-3-540-74686-7_8

for irreversible processes entropy has to increase, he could also calculate transport properties of the gas, for instance, its heat conductivity or its viscosity.

In the original form, the BE holds only for dilute, neutral gases with a short range interaction, for which $nR^3 \ll 1$, where n is the density of the gas and R is the range of the interaction potential. However, it has also been applied to physical systems, for which, at first sight, the condition $nR^3 \ll 1$ is not satisfied. For instance, the kinetic description of plasmas in laboratory gas discharges or interstellar clouds is usually based on a BE, although $R \to \infty$ for the Coulomb interaction. Thus, $nR^3 \ll 1$ cannot be satisfied, for any density. A careful study of the Coulomb collision integral showed, however, that the bare Coulomb interaction has to be replaced by the screened one, resulting in a modified BE, the Lenard-Balescu equation [2, 3], which can then indeed be employed for the theoretical analysis of plasmas [4, 5].

In the temperature and density range of interest, ionized gases are, from a statistical point of view, classical systems. The technical problems due to the Coulomb interaction not withstanding, it is therefore clear that a BE, which obviously belongs to the realm of classical statistical mechanics, can be in principle formulated for a plasma.

The BE has also been successfully applied to condensed matter, in particular, to quantum fluids, metals, and semiconductors [6, 7, 8], whose microscopic description has to be quantum-mechanical. Hence, transport properties of these systems should be calculated quantum-statistically, using a quantum-kinetic equation, instead of a BE [9, 10, 11]. In addition, naively, one would not expect the condition $nR^3 \ll 1$ to be satisfied. The densities of condensed matter are too high. A profound quantum-mechanical analysis in the first half of the 20^{th} century [12, 13, 14] revealed, however, that the carriers in condensed matter are not the tightly bound, dense building blocks but physical excitation which, at a phenomenological level, resemble a dilute gas of *quasiparticles* for which a BE or a closely related kinetic equation can indeed be formulated.

The quasiparticle concept opens the door for Boltzmann transport in condensed matter, see Fig. 8.1. Depending on the physical system, electrons or ion cores in a solid, normal or superfluid/superconducting quantum fluids etc., various types of quasiparticles can be defined quantum-mechanically, whose kinetics can then be modelled by an appropriate semi-classical BE. Its mathematical structure, and with it the solution strategy, is essentially independent of the physical context. Below, we restrict ourselves to the transport resulting from electronic quasiparticles in a crystal. Further examples of semi-classical quasiparticle transport can be found in the excellent textbook by Smith and Jensen [7].

8.1.2 Electronic Quasiparticles in a Crystal

To facilitate a qualitative understanding of the quasiparticle concept as applied to electrons, we recall the quantum mechanics of a single electron in a crystal. Writing the electrons' wave function in Bloch form $\psi_{n\boldsymbol{k}}(\boldsymbol{r}) = \mathrm{e}^{\mathrm{i}\boldsymbol{k}\cdot\boldsymbol{r}} u_{n\boldsymbol{k}}(\boldsymbol{r})/\sqrt{V}$ with

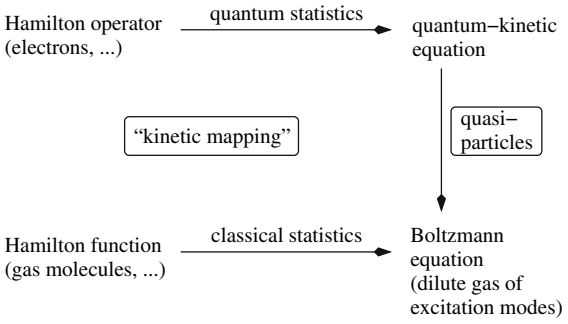

Fig. 8.1. This cartoon puts the content of this chapter into perspective. For neutral or ionized gases, the BE and its range of validity, can be directly derived from the Hamilton function for the classical gas molecules. In that case, the BE determines the distribution function for the constituents of the physical system under consideration. In the context of condensed matter, however, the BE describes the distribution function for the excitation modes (quasiparticles) and not for the constituents (electrons, ion cores, ...) although the BE has to be obtained – by quantum-statistical means – from the constituents' Hamilton operator. The definition of quasiparticles is absolutely vital for setting-up a BE. It effectively maps, as far as the kinetics is concerned, the quantum-mechanical many-particle system of the constituents to a semi-classical gas of excitation modes

an appropriately normalized, lattice periodic Bloch function[1] $u_{n\boldsymbol{k}}$, the one-particle Schrödinger equation, which determines the quasiparticle energies $E_n(\boldsymbol{k})$ with n the band index and $\boldsymbol{k}$ the wave vector in the first Brillouin zone, is given by

$$\left[\frac{\hbar^2(\nabla+\mathrm{i}\boldsymbol{k})^2}{2m_e}+V(\boldsymbol{r})\right]u_{n\boldsymbol{k}}(\boldsymbol{r})=E_n(\boldsymbol{k})u_{n\boldsymbol{k}}(\boldsymbol{r}) - \int \mathrm{d}\boldsymbol{r}'\Sigma(\boldsymbol{r}-\boldsymbol{r}',E_n(\boldsymbol{k}))\mathrm{e}^{\mathrm{i}\boldsymbol{k}\cdot(\boldsymbol{r}'-\boldsymbol{r})}u_{n\boldsymbol{k}}(\boldsymbol{r}')\;, \quad (8.2)$$

where we separated the lattice-periodic potential $V(\boldsymbol{r})$ originating from the rigidly arranged ion cores from the energy dependent potential $\Sigma(\boldsymbol{r},E)$ (self-energy) which arises from the coupling to other charge carriers as well as to the ion cores' deviations from the equilibrium positions (phonons).

Let us first consider (8.2) for $\Sigma=0$. An electron moving through the crystal experiences then only the lattice periodic potential V. It gives rise to extremely strong scattering, with a mean free path of the order of the lattice constant, which could never be treated in the framework of a BE. However, this scattering is not random. It originates from the periodic array of the ion cores and leads to the formation of bare energy bands. Within these bands, the motion of the electron is coherent, but with a dispersion which differs from the dispersion of a free electron. Because of

[1] The Bloch functions are orthonormal when integrated over a unit cell v_{cell} : $v_{\mathrm{cell}}^{-1}\int_{\mathrm{cell}}\mathrm{d}\boldsymbol{r}\;u_{n\boldsymbol{k}}(\boldsymbol{r})^*u_{n'\boldsymbol{k}'}(\boldsymbol{r})=\delta_{nn'}\delta_{\boldsymbol{k},\boldsymbol{k}'}$.

this difference, the electron no longer sees the rigid array of ion cores. Its mean free path exceeds therefore the lattice constant, and a BE may become feasible.

However, in a crystal there is not only one electron but many, and the lattice of ion cores is not rigid but dynamic. Thus, electron-electron and electron-phonon interaction have to be taken into account giving rise to $\Sigma \neq 0$. As a result, the Schrödinger equation (8.2) becomes an implicit eigenvalue problem for the renormalized energy bands $E_n(\boldsymbol{k})$ which may contain a real and an imaginary part. For the purpose of the discussion, we assume Σ to be real. Physically, the dressing of the electron incorporated in Σ arises from the fact that the electron attracts positively charged ion cores and repels other electrons, as visualized in Fig. 8.2. The former gives rise to a lattice distortion around the considered electron and the latter leads to a depletion of electrons around it[2].

While coherent scattering on the periodic array of ion cores transforms bare electrons into band electrons, which is favorable for a BE description, residual interactions turn band electrons into dressed quasiparticles, which may be detrimental to it, because the dressing is energy and momentum dependent. Quasiparticles are therefore complex objects. Nevertheless, they are characterized by a dispersion, carry a negative elementary charge, and obey Fermi statistics, very much like band electrons. Provided they are well-defined, which means that the imaginary part of Σ, which we neglected so far in our discussion, is small compared to the real part of Σ, a BE may be thus also possible for them. However, the justification of the

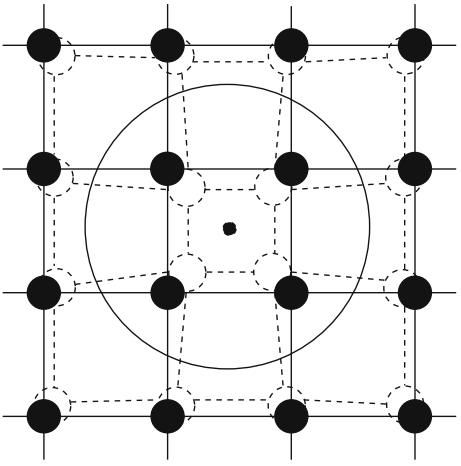

Fig. 8.2. Graphical representation of the many-body effects contained in the selfenergy Σ. The lattice distortion (*dashed lines*) and the depletion region (*large solid circle*) turn bare band electrons (*visualized by the small bullet*) into quasiparticles which carry the lattice distortion and the depletion region with it when they move through the crystal

[2] Here, exchange effects are also important, because electrons are fermions. At a technical level, the depletion region is encoded in the Coulomb hole and the screened exchange selfenergy.

quasiparticle BE will be subtle. Indeed, there are no pre-canned recipes for this task. Each physical situation has to be analyzed separately, using quantum-statistical techniques [9, 10, 11].

For standard metals [15] and superconductors [16, 17, 18, 19], for instance, the BE for quasiparticles can be rigorously derived from basic Hamiltonians, provided the quasiparticles are well-defined. The main reason is the separation of energy scales [20]: A high-energy scale set by the Fermi momentum k_F and a low-energy scale given by the width Δk of the thermal layer around the Fermi surface, see Fig. 8.3. The latter also defines the wavelength $1/\Delta k$ of the quasiparticles responsible for transport. Because of the separation of scales, an ab initio calculation of transport coefficients is possible along the lines put forward by Rainer [21] for the calculation of transition temperatures in superconductors, which is a closely related problem, see also [22].

For semiconductors, on the other hand, a BE for quasiparticles can only be rigorously derived when they are degenerate, that is, heavily doped and thus metal-like; the scales are then again well separated. However, when the doping is small, or in moderately optically excited semiconductors, the electrons are non-degenerate. Thus, neither a Fermi energy nor a transport energy scale can be defined. In that case, a BE for quasiparticles is very hard to justify from first principles [23], despite the empirical success the BE has also in these situations.

8.1.3 Heuristic Derivation of the Quasiparticle Boltzmann Equation

Since we will be mainly concerned with computational techniques developed for the solution of the quasiparticle BE, we skip the lengthy quantum-statistical

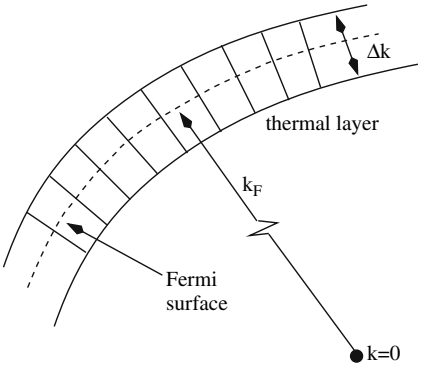

Fig. 8.3. Separation of the momentum (and thus energy) scales in a metal. The Fermi momentum k_F sets the high-energy scale, whereas the thermal smearing-out of the Fermi surface, Δk, gives the scale relevant for transport. Using quantum-statistical methods, a correlation function called g^K, which is closely related to the distribution function g can be systematically expanded in $\Delta k/k_F \sim kT/E_F$. If the quasiparticles have long enough lifetimes, g^K reduces, in leading order, to g and satisfies a BE [20]

derivation and simply summarize the necessary conditions a many-particle system has to satisfy to be suitable for a BE-based analysis:

(i) The quasiparticles should be well-defined objects. The time they spend in a state with energy $E_n(\boldsymbol{k})$, that is, the average time before scattering between quasiparticles, with material imperfections, or with phonons[3] takes place, should be large compared to $\hbar/E_n(\boldsymbol{k})$.
(ii) The coupling to the scatterer (impurities, quasiparticles, and phonons) should be weak, that is, the collision integral in the quasiparticle BE should be calculable perturbatively.
(iii) External electro-magnetic fields and temperature gradients should be weak enough so that their effect during a collision can be neglected. In addition, their spatio-temporal variation has to be small within a mean free path or a mean free time.

When conditions (i)–(iii) are satisfied, a BE exists for quasiparticles. This is the regime of Boltzmann transport in condensed matter.

The structure of the BE for quasiparticles can be guessed heuristically. In analogy to the BE (8.1), it should be an *equation of motion* for the quasiparticle distribution function in the n^{th} band, $g_n(\boldsymbol{r},\boldsymbol{k},t)$. Notice, instead of the velocity $\boldsymbol{v}$, the momentum $\boldsymbol{k}$ is now used, because $\boldsymbol{k}$ is the relevant one-particle quantum number in a given band. The distribution function contains both $\boldsymbol{r}$ and $\boldsymbol{k}$ as independent variables, whereas the uncertainty principle prohibits a simultaneous measurement of the two. Thus, by necessity, the quasiparticle BE has to be a rather subtle semi-classical equation.

Within the semi-classical framework, quasiparticles perform classical intra-band free flights and occasionally scatter on imperfections, phonons, or other quasiparticles, which then leads to transitions between momentum states and possibly between bands. Accordingly, the equation of motion which governs the free flight of a quasiparticle in an electro-magnetic field specified by a vector potential $\boldsymbol{A}$ and a scalar potential U can be derived from the classical Hamiltonian [24]

$$\mathcal{H} = E_n\left(\frac{1}{\hbar}\boldsymbol{p} + \frac{e}{\hbar c}\boldsymbol{A}(\boldsymbol{r})\right) - eU(\boldsymbol{r})\ , \tag{8.3}$$

where $E_n(\boldsymbol{k})$ is the band energy obtained from the solution of the Schrödinger equation (8.2), $\hbar\boldsymbol{k}$ is the kinetic momentum, and $\boldsymbol{p}$ and $\boldsymbol{r}$ are, respectively, the canonical momentum and coordinate of the quasiparticle. From the Hamilton equations it then follows, that a quasiparticle in the n^{th} band centered at $\boldsymbol{r}$ and $\boldsymbol{k}$ in phase space has to move according to

[3] Naturally, phonons comprising the lattice distortion accounted for in the definition of quasiparticles do not lead to scattering. But there is a residual electron-phonon interaction which induces transitions between different quasiparticle states.

$$\left(\frac{\mathrm{d}\boldsymbol{r}}{\mathrm{d}t}\right)_n = \boldsymbol{v}_n(\boldsymbol{k}) = \frac{1}{\hbar}\nabla_{\boldsymbol{k}} E_n(\boldsymbol{k}) \,,$$
$$\left(\hbar\frac{\mathrm{d}\boldsymbol{k}}{\mathrm{d}t}\right)_n = \boldsymbol{F}_n = -e\left(\boldsymbol{E} + \frac{1}{c}\boldsymbol{v}_n(\boldsymbol{k}) \times \boldsymbol{B}\right) \tag{8.4}$$

with $\boldsymbol{E} = -\nabla_{\boldsymbol{r}} U$ and $\boldsymbol{B} = \nabla_{\boldsymbol{r}} \times \boldsymbol{A}$, which immediately leads to the quasiparticle BE

$$\frac{\partial g_n}{\partial t} + \boldsymbol{v}_n \cdot \nabla_{\boldsymbol{r}} g_n - \frac{e}{\hbar}\left(\boldsymbol{E} + \frac{1}{c}\boldsymbol{v}_n \times \boldsymbol{B}\right) \cdot \nabla_{\boldsymbol{k}} g_n = \left(\frac{\partial g_n}{\partial t}\right)_c \,, \tag{8.5}$$

when the time evolutions of the distribution function due to streaming (l.h.s.) and scattering (r.h.s.) are balanced.

Suppressing the variables $\boldsymbol{r}$ and t, the general structure of the collision integral is

$$\left(\frac{\partial g_n}{\partial t}\right)_c = \sum_{n'\boldsymbol{k}'} \{S_{n'\boldsymbol{k}',n\boldsymbol{k}} g_{n'}(\boldsymbol{k}')[1 - g_n(\boldsymbol{k})] - S_{n\boldsymbol{k},n'\boldsymbol{k}'} g_n(\boldsymbol{k})[1 - g_{n'}(\boldsymbol{k}')]\} \tag{8.6}$$

with $S_{n'\boldsymbol{k}',n\boldsymbol{k}}$ the probability for scattering from the quasiparticle state $n'\boldsymbol{k}'$ to the quasiparticle state $n\boldsymbol{k}$, which has to be determined from the quantum mechanics of scattering. Its particular form depends on the scattering process (see below). The collision integral consists of two terms: The term proportional to $1 - g_n(\boldsymbol{k})$ accounts for scattering-in (gain) processes, whereas the term proportional to $g_n(\boldsymbol{k})$ takes scattering-out (loss) processes into account. Note, for non-degenerate quasiparticles[4], $g_n(\boldsymbol{k}) \ll 1$ and the Pauli-blocking factor $1 - g_n(\boldsymbol{k})$ reduces to unity.

Some of the numerical techniques we will discuss below are tailored for the solution of the steady-state, spatially uniform, linearized quasiparticle BE, applicable to situations, where the external fields are weak and the system is close to thermal equilibrium. This equation can be obtained from the full BE (8.5) through an expansion around thermal equilibrium. In the absence of magnetic fields and for a single band it reads [6, 7]

$$-e\boldsymbol{E} \cdot \boldsymbol{v} \left.\frac{\partial f}{\partial E}\right|_{E(\boldsymbol{k})} = \left(Cg^{(1)}\right)(\boldsymbol{k}) \,, \tag{8.7}$$

where the r.h.s. symbolizes the linearized collision integral and $g^{(1)} = g - f$ is the deviation of the distribution function from the Fermi function $f(E) = [\exp(E/k_{\mathrm{B}}T) + 1]^{-1}$. Here T is the temperature and E measures the energy from the chemical potential. With the help of the detailed balance condition

$$S_{\boldsymbol{k}',\boldsymbol{k}} f(E(\boldsymbol{k}'))[1 - f(E(\boldsymbol{k}))] = S_{\boldsymbol{k},\boldsymbol{k}'} f(E(\boldsymbol{k}))[1 - f(E(\boldsymbol{k}'))] \,, \tag{8.8}$$

the linearized collision integral becomes[5]

[4] Quasiparticles with mass m^* are non-degenerate when $n\lambda_{dB}^3 \ll 1$, where n is the density and $\lambda_{dB} = \sqrt{h^2/2\pi m^* k_{\mathrm{B}} T}$ is the de Broglie wavelength of the quasiparticles.

[5] Recall, we suppress in the collision integral the variables $\boldsymbol{r}$ and t.

$$\begin{aligned}\left(Cg^{(1)}\right)(\boldsymbol{k}) &= \sum_{\boldsymbol{k}'} S_{\boldsymbol{k},\boldsymbol{k}'} \left\{ g^{(1)}(\boldsymbol{k}') \frac{f(E(\boldsymbol{k}))}{f(E(\boldsymbol{k}'))} - g^{(1)}(\boldsymbol{k}) \frac{1-f(E(\boldsymbol{k}'))}{1-f(E(\boldsymbol{k}))} \right\} \\ &= \sum_{\boldsymbol{k}'} \widetilde{Q}_{\boldsymbol{k},\boldsymbol{k}'} g^{(1)}(\boldsymbol{k}') \ , \end{aligned} \tag{8.9}$$

where in the second line we defined a matrix

$$\widetilde{Q}_{\boldsymbol{k},\boldsymbol{k}'} = S_{\boldsymbol{k},\boldsymbol{k}'} \frac{f(E(\boldsymbol{k}))}{f(E(\boldsymbol{k}'))} - \sum_{\boldsymbol{k}''} S_{\boldsymbol{k}',\boldsymbol{k}''} \frac{1-f(E(\boldsymbol{k}''))}{1-f(E(\boldsymbol{k}'))} \delta_{\boldsymbol{k}\boldsymbol{k}'} \ . \tag{8.10}$$

8.2 Techniques for the Solution of the Boltzmann Equation

In the previous section we phenomenologically derived the BE for quasiparticles[6] and listed the necessary conditions for Boltzmann transport in condensed matter. The standard way to analyze transport processes in condensed matter consists then of three main steps:

(i) Determine appropriate interaction mechanisms for the quasiparticles responsible for the transport phenomenon under consideration and calculate the relevant scattering probabilities. This step requires quasiparticle energies and wave functions. For electronic quasiparticles, they have to be obtained from (8.2) using, for instance, the ab initio methods described in Chap. 14.
(ii) Write down the BE in terms of the external driving terms and scattering probabilities and solve it.
(iii) Calculate the relevant currents for a confrontation with experiments. For weak external fields, i.e., in the linear regime, use the currents to extract transport coefficients (electric and thermal conductivity, mobility etc.) which may be more suitable for a comparison with experiments.

The calculation of the currents or transport coefficients is straightforward provided the solution of the BE is known. Solving the BE is, however, a serious task. It is a complicated non-linear integro-differential equation, which in almost all cases of interest cannot be solved analytically. Noteworthy exceptions are the linearized BE for a classical gas with an interaction potential $U(r) \sim r^{-4}$ [7] and the linearized BE for an isotropic Fermi liquid at very low temperatures, where particle-particle Coulomb scattering dominates [25, 26].

Usually the BE has to be solved with a computer. Two groups of techniques can be roughly distinguished. The first group consists of *classical* numerical techniques for the solution of integro-differential equations (approximating differentials by finite differences, integrals by sums, and using numerical routines for manipulating the resulting algebraic equations). They are mostly applied to situations where external fields and temperature gradients are weak and the BE can be linearized around the local thermal equilibrium. In principle, however, they can be also used to solve

[6] From now on, BE refers to quasiparticle BE.

the full BE. With an eye on the calculation of the electric conductivity of metals and the calculation of hot-electron distributions in semiconductors, we will describe two such methods: Numerical iteration [27, 28, 29, 30, 31, 32, 33, 34, 35] and *algebraization* through an expansion of the distribution function in terms of a set of basis functions [36, 37, 38, 39, 40, 41, 42, 43].

The second group consists of Monte Carlo techniques for the direct simulation of the stochastic motion of quasiparticles, whose distribution function is governed by the BE. These techniques are the most popular ones currently used because the concepts they invoke are easy to grasp and straightforward to implement on a computer. In addition, Monte Carlo techniques can be applied to far-off-equilibrium situations and are thus ideally suited for studying hot-electron transport in semiconductor devices which is of particular importance for the micro-electronics industry. Below, we will present two different Monte Carlo approaches. The first approach, which evolved into a design tool for electronic circuit engineers, samples the phase space of the quasiparticles by monitoring the time evolution of a single test-particle [44, 45, 46, 47, 48, 49]. Whereas the second approach generates the time evolution of N-electron configurations in a discretized momentum space [50]. This is particularly useful for degenerate electrons, where Pauli-blocking is important.

8.2.1 Numerical Iteration

8.2.1.1 Spatially Uniform, Steady-State BE with Linearized Collision Integral

Based on the linearized BE (8.7), numerical iteration has been extensively used for calculating steady-state transport coefficients for metals in uniform external fields [27, 28, 29, 30]. In contrast to the full BE, the linearized BE is not an integro-differential equation but an inhomogeneous integral equation to which an iterative approach can be directly applied. As an illustration, we consider the calculation of the electric conductivity tensor $\boldsymbol{\sigma}$.

To set up the iteration scheme, $g^{(1)}$ is written in a form which anticipates that $g^{(1)}$ will change rapidly in the vicinity of the Fermi surface, see Fig. 8.3, while it will be a rather smooth function elsewhere. The relaxation time approximation [6, 7] suggests for $g^{(1)}$ the ansatz

$$g^{(1)}(\boldsymbol{k}) = -\frac{\partial f}{\partial E}\bigg|_{E(\boldsymbol{k})} e\boldsymbol{E}\cdot\boldsymbol{v}(\boldsymbol{k})\phi(\boldsymbol{k}) \;, \tag{8.11}$$

where $E(\boldsymbol{k})$ and $\boldsymbol{v}(\boldsymbol{k})$ are, respectively, the energy measured from the chemical potential and the group velocity of the quasiparticles. In terms of the function $\phi(\boldsymbol{k})$, which can be interpreted as a generalized, $\boldsymbol{k}$-dependent relaxation time, the electric current becomes [6, 7]

$$\boldsymbol{j} = 2e\int \frac{\mathrm{d}\boldsymbol{k}}{(2\pi)^3}\,\boldsymbol{v}(\boldsymbol{k})\; g^{(1)}(\boldsymbol{k})$$

$$= -2e^2 \int \frac{\mathrm{d}\boldsymbol{k}}{(2\pi)^3}\, \phi(\boldsymbol{k})\, \frac{\partial f}{\partial E}\bigg|_{E(\boldsymbol{k})} \boldsymbol{v}(\boldsymbol{k}) : \boldsymbol{v}(\boldsymbol{k})\boldsymbol{E}$$
$$= \boldsymbol{\sigma}\boldsymbol{E}\ , \tag{8.12}$$

from which we can read off the electric conductivity tensor

$$\boldsymbol{\sigma} = -2e^2 \int \frac{\mathrm{d}\boldsymbol{k}}{(2\pi)^3}\, \phi(\boldsymbol{k})\, \frac{\partial f}{\partial E}\bigg|_{E(\boldsymbol{k})} \boldsymbol{v}(\boldsymbol{k}) : \boldsymbol{v}(\boldsymbol{k})\ , \tag{8.13}$$

where : denotes the tensor product and the factor two comes from the spin. Note, although the particular structure of (8.11) is inspired by the relaxation time approximation, the iterative approach goes beyond it, because it does not replace the linearized collision integral by $-g^{(1)}/\tau$, where τ is the relaxation time, but keeps it fully intact. In addition, it is also more general than variational approaches [6, 7] because the function $\phi(\boldsymbol{k})$ is left unspecified.

To proceed, we insert (8.11) into (8.7). Using the collision integral in the form (8.9) and defining

$$X(\boldsymbol{k};\boldsymbol{E}) = -e\boldsymbol{E}\cdot\boldsymbol{v}(\boldsymbol{k})\ , \tag{8.14}$$

we obtain

$$X(\boldsymbol{k};\boldsymbol{E})\frac{\partial f}{\partial E}\bigg|_{E(\boldsymbol{k})} = \sum_{\boldsymbol{k}'} S_{\boldsymbol{k},\boldsymbol{k}'} \left[\frac{1-f(E(\boldsymbol{k}'))}{1-f(E(\boldsymbol{k}))} \frac{\partial f}{\partial E}\bigg|_{E(\boldsymbol{k})} X(\boldsymbol{k};\boldsymbol{E})\phi(\boldsymbol{k}) \right.$$
$$\left. - \frac{f(E(\boldsymbol{k}))}{f(E(\boldsymbol{k}'))} \frac{\partial f}{\partial E}\bigg|_{E(\boldsymbol{k}')} X(\boldsymbol{k}';\boldsymbol{E})\phi(\boldsymbol{k}') \right]\ , \tag{8.15}$$

which can be simplified to

$$\phi(\boldsymbol{k}) = \frac{1 + \sum_{\boldsymbol{k}'} S_{\boldsymbol{k},\boldsymbol{k}'} \frac{[1-f(E(\boldsymbol{k}'))]X(\boldsymbol{k}';\boldsymbol{E})}{[1-f(E(\boldsymbol{k}))]X(\boldsymbol{k};\boldsymbol{E})}\phi(\boldsymbol{k}')}{\sum_{\boldsymbol{k}'} S_{\boldsymbol{k},\boldsymbol{k}'} \frac{1-f(E(\boldsymbol{k}'))}{1-f(E(\boldsymbol{k}))}}\ , \tag{8.16}$$

when we recall the identity

$$\frac{\partial f}{\partial E}\bigg|_{E(\boldsymbol{k})} = \frac{1}{k_{\mathrm{B}}T} f(E(\boldsymbol{k}))[1-f(E(\boldsymbol{k}))]\ . \tag{8.17}$$

Notice that the precise form of the single band scattering probability $S_{\boldsymbol{k},\boldsymbol{k}'}$ is immaterial for the iteration procedure which can thus handle all three major scattering processes: Elastic electron-impurity, inelastic electron-phonon, and electron-electron scattering.

Equation (8.16) is an inhomogeneous integral equation suitable for iteration: Starting with $\phi^{(0)} = 0$ (thermal equilibrium), a sequence of functions $\phi^{(i)}$, $i \geq 1$, can be successively generated, which comes with increasing i arbitrarily close to the exact solution, provided the process converges. Convergence is only guaranteed when the kernel is positive and continuous. This is not necessarily the case, but it can be enforced when selfscattering processes are included, see below.

The iteration process needs as an input the scattering probability. The most important scattering processes affecting the electric conductivity of metals are electron-impurity and electron-phonon scattering. The former determines the conductivity at low temperatures whereas the latter at high temperatures[7]. In our notation, these two scattering probabilities are given by [28]

$$S^{\text{imp}}_{\boldsymbol{k},\boldsymbol{k}'} = \frac{2\pi}{\hbar}|M^{\text{imp}}(\cos\theta_{\boldsymbol{k}\boldsymbol{k}'})|^2\delta(E(\boldsymbol{k}') - E(\boldsymbol{k}))\ , \tag{8.18}$$

$$\begin{aligned} S^{\text{ph}}_{\boldsymbol{k},\boldsymbol{k}'} = \frac{2\pi}{\hbar}\sum_{\boldsymbol{q}\lambda}\sum_{\boldsymbol{Q}_i}\left|M^{\text{ph}}_{\lambda}(\boldsymbol{k}'-\boldsymbol{k})\right|^2\big\{&N_{\lambda\boldsymbol{q}}\delta(E(\boldsymbol{k}') - E(\boldsymbol{k}) - \hbar\omega_{\lambda\boldsymbol{q}})\ \delta_{\boldsymbol{k}'-\boldsymbol{k},\boldsymbol{q}+\boldsymbol{Q}_i} \\ &+[1+N_{\lambda\boldsymbol{q}}]\ \delta(E(\boldsymbol{k}') - E(\boldsymbol{k}) + \hbar\omega_{\lambda\boldsymbol{q}})\delta_{\boldsymbol{k}-\boldsymbol{k}',\boldsymbol{q}+\boldsymbol{Q}_i}\big\}\ , \end{aligned} \tag{8.19}$$

where $M^{\text{imp}}(\cos\theta_{\boldsymbol{k}\boldsymbol{k}'})$ is the electron-impurity coupling which depends on the angle $\theta_{\boldsymbol{k}\boldsymbol{k}'}$ between $\boldsymbol{k}$ and $\boldsymbol{k}'$ (isotropic elastic scattering), $M^{\text{ph}}_{\lambda}(\boldsymbol{k}'-\boldsymbol{k})$ is the electron-phonon coupling, and $N_{\lambda\boldsymbol{q}} = [\exp(\hbar\omega_{\lambda\boldsymbol{q}}) - 1]^{-1}$ is the equilibrium distribution function for phonons with frequency $\omega_{\lambda\boldsymbol{q}}$; $\boldsymbol{q}$, λ, and $\boldsymbol{Q}_i$ are the phonon wave-vector, the phonon polarization, and the i^{th} reciprocal lattice vector, respectively. The coupling functions are material specific and can be found in the literature [6, 7, 8].

In order to obtain a numerically feasible integral equation, (8.18) and (8.19) are inserted into (8.16) and the momentum sums are converted into integrals. The integral over $\boldsymbol{k}'$ is then transformed into an integral over constant energy surfaces using[8]

$$\sum_{\boldsymbol{k}'} \to \int \frac{\mathrm{d}\boldsymbol{k}'}{(2\pi)^3} \to \frac{1}{(2\pi)^3}\int \mathrm{d}E(\boldsymbol{k}')\int \frac{\mathrm{d}\Omega(\boldsymbol{k}')}{\hbar|\boldsymbol{v}(\boldsymbol{k}')|}\ , \tag{8.20}$$

where $\mathrm{d}\Omega(\boldsymbol{k}')$ is the surface element on the energy surface $E(\boldsymbol{k}')$. The δ-functions appearing in the scattering probabilities (8.18) and (8.19) are then utilized to eliminate some of the integrations thereby reducing the dimensionality of (8.16). For isotropic bands $\phi(\boldsymbol{k}) \to \phi(E(\boldsymbol{k}))$, and one ends up with an one-dimensional integral equation which can be readily solved by iteration. For more details see [27, 28, 29, 30].

8.2.1.2 Spatially Uniform BE with the Full Collision Integral

The iterative approach can be also applied to the full BE. This is of particular interest for the calculation of distribution functions for electrons in strong external fields [31, 32, 33, 34, 35]. In that case, however, the BE has to be first converted into an integral equation. This is always possible because the free streaming term in (8.5) has the form of a total differential which can be integrated along its characteristics.

[7] Electron-electron scattering does not affect the electric conductivity, as long as normal processes are only taken into account. Umklapp processes, on the other hand, contribute to the conductivity, but the matrix elements are usually very small.

[8] The volume is put equal to one.

As an illustration, we consider a spatially uniform, non-degenerate electron system[9] in a single band and an arbitrarily strong electric field. Then we can write the BE as

$$\left\{\frac{\partial}{\partial t}-\frac{e}{\hbar}\boldsymbol{E}\cdot\nabla_{\boldsymbol{k}}+\lambda_{\boldsymbol{k}}+S_{\boldsymbol{k}}\right\}g(\boldsymbol{k},t)=\sum_{\boldsymbol{k}'}[S_{\boldsymbol{k}',\boldsymbol{k}}+S_{\boldsymbol{k}}\delta_{\boldsymbol{k},\boldsymbol{k}'}]g(\boldsymbol{k}',t)\ , \quad (8.21)$$

where we introduced the scattering-out rate

$$\lambda_{\boldsymbol{k}}=\sum_{\boldsymbol{k}'}S_{\boldsymbol{k},\boldsymbol{k}'}\ , \quad (8.22)$$

and added on both sides of the equation a selfscattering term $S_{\boldsymbol{k}}g(\boldsymbol{k},t)$, which has no physical significance, but is later needed to simplify the kernel of the integral equation.

To transform (8.21) into an integral equation, we introduce path variables $\boldsymbol{k}^*=\boldsymbol{k}+e/\hbar\boldsymbol{E}t^*$ and $t^*=t$ which describe the collisionless motion of the electrons along the characteristics of the differential operator [31, 45][10]. In terms of these variables, (8.21) can be written as

$$\frac{\mathrm{d}}{\mathrm{d}t^*}\left\{g(\boldsymbol{k}(\boldsymbol{k}^*,t^*),t^*)\,\mathrm{e}^{\int_0^{t^*}\mathrm{d}y\widetilde{\boldsymbol{\lambda}}_{\boldsymbol{k}(\boldsymbol{k}^*,y)}}\right\}=\mathrm{e}^{\int_0^{t^*}\mathrm{d}y\widetilde{\boldsymbol{\lambda}}_{\boldsymbol{k}(\boldsymbol{k}^*,y)}}\sum_{\boldsymbol{k}'}\widetilde{S}_{\boldsymbol{k}',\boldsymbol{k}(\boldsymbol{k}^*,t^*)}g(\boldsymbol{k}',t^*) \quad (8.23)$$

with $\widetilde{\boldsymbol{\lambda}}_{\boldsymbol{k}}=\lambda_{\boldsymbol{k}}+S_{\boldsymbol{k}}$ and $\widetilde{S}_{\boldsymbol{k}',\boldsymbol{k}}=S_{\boldsymbol{k}',\boldsymbol{k}}+S_{\boldsymbol{k}}\delta_{\boldsymbol{k}\boldsymbol{k}'}$. Integrating this equation from t_1^* to $t_2^*>t_1^*$ and setting $\boldsymbol{k}=\boldsymbol{k}^*-e\boldsymbol{E}t_2^*/\hbar$, $t=t_2^*$, and $t'=t_1^*$ yields

$$\begin{aligned}g(\boldsymbol{k},t)=&g\left(\boldsymbol{k}+\frac{e\boldsymbol{E}}{\hbar}(t-t'),t'\right)\mathrm{e}^{-\int_{t'}^{t}\mathrm{d}y\widetilde{\boldsymbol{\lambda}}_{\boldsymbol{k}+e\boldsymbol{E}(t-y)/\hbar}}\\&+\int_{t'}^{t}\mathrm{d}t^*\sum_{\boldsymbol{k}'}\mathrm{e}^{-\int_{t^*}^{t}\mathrm{d}y\widetilde{\boldsymbol{\lambda}}_{\boldsymbol{k}+e\boldsymbol{E}(t-y)/\hbar}}\ \widetilde{S}_{\boldsymbol{k}',\boldsymbol{k}+e\boldsymbol{E}(t-t^*)/\hbar}\ g(\boldsymbol{k}',t^*)\ . \quad (8.24)\end{aligned}$$

This equation, which is an integral representation of the BE (8.21), can be further simplified when we consider the physical content of the terms on the r.h.s. The first term denotes the contribution to $g(\boldsymbol{k},t)$ originating from electrons which were in state $\boldsymbol{k}+e\boldsymbol{E}(t-t')/\hbar$ at time t' and drifted to the state $\boldsymbol{k}$ at time t without being scattered. The second term, on the other hand, denotes the contribution of electrons which were scattered from any state $\boldsymbol{k}'$ to the new state $\boldsymbol{k}+e\boldsymbol{E}(t-t^*)/\hbar$ at any time t^* between t and t' and arrive at the state $\boldsymbol{k}$ at time t without being scattered. In both terms, the time t' is arbitrary. It can be any time. The only requirement is that $t'<t$. We can thus take the convenient limit $t'\to-\infty$, in which case the first term on the r.h.s. of (8.24) vanishes because $g(\boldsymbol{k},t)$ vanishes for $\boldsymbol{k}\to\infty$. The integral representation of (8.21) reduces therefore to

[9] No Pauli blocking, i.e. $1-g\to1$ in (8.6).

[10] A generalization of the procedure to spatially non-uniform situations is conceivable, but will not be discussed here.

$$g(\boldsymbol{k},t) = \int\limits_{-\infty}^{t} \mathrm{d}t^* \sum_{\boldsymbol{k}'} \mathrm{e}^{-\int_{t^*}^{t} \mathrm{d}y \widetilde{\lambda}_{\boldsymbol{k}+e\boldsymbol{E}(t-y)/\hbar}} \widetilde{S}_{\boldsymbol{k}',\boldsymbol{k}+e\boldsymbol{E}(t-t^*)/\hbar}\, g(\boldsymbol{k}',t^*)\,. \quad (8.25)$$

This form of the BE is not yet particularly useful, because the time integral in the exponent contains an integrand which almost always cannot be integrated exactly. Even if it can, the result would be a complicated function, unsuited for fast numerical manipulations. It is at this point, where the selfscattering term, which we artificially added on both sides of the BE, can be used to dramatically simplify the integral equation, as was first noticed by Rees [32]. Since the selfscattering rate $S_{\boldsymbol{k}}$ is completely unspecified, we can use it to enforce a particularly simple form of $\widetilde{\lambda}_{\boldsymbol{k}}$. An obvious choice is

$$\widetilde{\lambda}_{\boldsymbol{k}} = \lambda_{\boldsymbol{k}} + S_{\boldsymbol{k}} = \Gamma \equiv \text{const} \quad (8.26)$$

with a constant $\Gamma > \sup \lambda_{\boldsymbol{k}}$ in order to maintain the physical desirable interpretation of $S_{\boldsymbol{k}} = \Gamma - \lambda_{\boldsymbol{k}}$ in terms of a selfscattering rate, which, of course, has to be positive. With (8.26), (8.25) reduces after a re-labeling of the time integration variable to

$$g(\boldsymbol{k},t) = \int\limits_{0}^{\infty} \mathrm{d}\tau \sum_{\boldsymbol{k}'} \mathrm{e}^{-\Gamma\tau} \widetilde{S}_{\boldsymbol{k}',\boldsymbol{k}+e\boldsymbol{E}\tau/\hbar} g(\boldsymbol{k}',t-\tau)\,. \quad (8.27)$$

This form of the uniform BE is well-suited for an iterative solution [32, 34]. The parameter Γ turns out to be crucial. It not only eliminates a complicated integration but it also enforces a positive, continuous kernel which is necessary for the iteration procedure to converge [33].

From a numerical point of view, integral equations are less prone to numerical errors than differential equations. It can be therefore expected that an iteration based solution of (8.27) is numerically more robust than a numerical treatment of the BE in integro-differential form. Another nice property of the iterative approach is that it processes the whole distribution function which is available any time during the calculation. This is particularly useful for degenerate electrons, where Pauli-blocking affects electron-electron and electron-phonon scattering rates. In the simplest, and thus most efficient, particle-based Monte Carlo simulations, in contrast, the distribution function is only available at the end of the simulation, see Sect. 8.2.3.

At first sight the dimensionality of the integral equation[11] seems to ruin any efficient numerical treatment of (8.27). This is however not necessarily so. The time integration, for instance, is a convolution and can be eliminated by a Laplace transform ($t \leftrightarrow s$). In the Laplace domain, (8.27) contains s only as a parameter not as an integration variable. The efficiency of the method depends then on the efficiency with which the remaining $\boldsymbol{k}$-integration can be performed. For realistic band structures and scattering processes this may be time consuming. However, it is always possible to express $g(\boldsymbol{k},s)$ in a symmetry adopted set of basis functions, thereby converting (8.27) into a set of integral equations with lower dimensionality.

[11] Three momentum variables and one time variable.

Hammar [35], for instance, used Legendre polynomials to expand the angle dependence of the distribution function and obtained an extremely fast algorithm for the calculation of hot-electron distributions in $p - Ge$ and $n - GaAs$. In addition, it is conceivable to construct approximate kernels, which are numerically easier to handle.

8.2.2 Expansion into an Orthonormal Set of Basis Functions

Another technique which is often used to solve the BE is the expansion of the one-particle distribution function in terms of an orthonormal set of basis functions. The BE reduces then to a set of integro-differential equations with less independent variables. The method leads thus to a partial algebraization of the BE.

A typical example from plasma physics is the Lorentz ansatz for the distribution function

$$g(\boldsymbol{r}, \boldsymbol{v}, t) = g^{(0)}(\boldsymbol{r}, v, t) + \boldsymbol{g}^{(1)}(\boldsymbol{r}, v, t) \cdot \frac{\boldsymbol{v}}{v} + ... \tag{8.28}$$

which comprises the first two terms of the expansion of the velocity space angle dependence of $g(\boldsymbol{r}, \boldsymbol{v}, t)$ in terms of spherical harmonics. In particular, calculations of transport coefficients for gas discharges are based on this expansion, see, for instance, the review by Winkler [5]. The simplification arises here from the fact that the expansion coefficients $g^{(i)}$ with $i = 0, 1, ...$ are independent of the angle variables in velocity space. Hence, the equations determining $g^{(i)}$, which are obtained from the BE by inserting (8.28) and averaging over the velocity space angles, have two less independent variables. Symmetries of the discharge can be used to further reduce the number of independent variables. This depends, however, on the details of the discharge and thus on the particular form of the BE.

Naturally, the expansion method is most useful for the spatially-uniform, steady-state, linearized BE, where the expansion coefficients depend at most on the magnitude of the velocity and the collision integral is linear in the expansion coefficients. As an example from condensed matter physics, we discuss here the expansion method developed by Allen [37] and Pinski [38]. It is an adaptation of (8.28) to quasiparticles and has been applied to various metals and alloys [39, 40, 41, 42, 43]. In that case, the *algebraization* is even complete leading to a linear set of algebraic equations for the expansion coefficients, which are just constants. In addition, the Allen-Pinski expansion typifies an ab initio approach because it is usually furnished with first-principle electronic structure data.

Having in mind the calculation of the electric conductivity of a metal, we again start from the linearized BE (8.7), but now with the linearized collision integral written in the form (8.9). Defining the function ϕ by

$$g^{(1)}(\boldsymbol{k}) = -\frac{\partial f}{\partial E}\bigg|_{E(\boldsymbol{k})} \phi(\boldsymbol{k}) \,, \tag{8.29}$$

which deviates slightly from the definition used in the previous subsection, and assuming the electric field to be in x-direction, the electric current in x-direction becomes, see (8.12),

$$j_x = -2e \sum_{\boldsymbol{k}} v_x(\boldsymbol{k}) \frac{\partial f}{\partial E}\bigg|_{E(\boldsymbol{k})} \phi(\boldsymbol{k}) \tag{8.30}$$

with ϕ satisfying the linearized BE in the form

$$-eE_x v_x(\boldsymbol{k}) \frac{\partial f}{\partial E}\bigg|_{E(\boldsymbol{k})} = \sum_{\boldsymbol{k}'} Q_{\boldsymbol{k}\boldsymbol{k}'} \phi(\boldsymbol{k}') \ , \tag{8.31}$$

where the kernel of the collision integral is given by

$$Q_{\boldsymbol{k}\boldsymbol{k}'} = -\frac{\partial f}{\partial E}\bigg|_{E(\boldsymbol{k})} \widetilde{Q}_{\boldsymbol{k}\boldsymbol{k}'} \tag{8.32}$$

with $\widetilde{Q}_{\boldsymbol{k}\boldsymbol{k}'}$ defined in (8.10).

Although the iterative approach described in the previous subsection could be used to calculate $\phi(\boldsymbol{k})$ from (8.31), this is not very efficient, in particular, for metals with a complicated Fermi surface, where the required numerical integrations can be rather subtle and time-consuming. Allen [37] suggested therefore to expand $\phi(\boldsymbol{k})$ in a complete set of functions, which takes the symmetry of the crystal and thus the topology of the Fermi surface into account, and to transform (8.31) to a symmetry-adapted matrix representation which is then solved by matrix inversion. For that purpose Allen [37] introduced a particular biorthogonal product basis, consisting of Fermi surface harmonics $F_J(\boldsymbol{k})$ and energy polynomials $\sigma_n(E(\boldsymbol{k}))$.

The strength of Allen's approach stems form the mathematical properties of the basis functions. The Fermi surface harmonics $F_J(\boldsymbol{k})$ with $J = X, Y, Z, X^2, ...$ are polynomials of the three Cartesian components of the velocity $\boldsymbol{v}(\boldsymbol{k})$. They are periodic functions in $\boldsymbol{k}$-space and orthogonal when integrated over the Fermi surface [36]. More precisely

$$\sum_{\boldsymbol{k}} F_J(\boldsymbol{k}) F_{J'}(\boldsymbol{k}) \delta(E(\boldsymbol{k}) - E) = N(E) \delta_{JJ'} \tag{8.33}$$

with $N(E) = \sum_{\boldsymbol{k}} \delta(E(\boldsymbol{k}) - E)$ the single-spin density of states at energy E; recall, we put the volume equal to one. Fermi surface harmonics are useful for the description of variations of $\phi(\boldsymbol{k})$ on the energy shell, which may be anisotropic and even consisting of various unconnected pieces. For spherical energy shells, the $F_J(\boldsymbol{k})$ reduce to spherical harmonics $Y_{lm}(\widehat{\boldsymbol{k}})$ with $\widehat{\boldsymbol{k}}$ the unit vector in direction of $\boldsymbol{k}$. For general topologies they have to be constructed on a computer. The Fermi surface harmonics transform as basis functions of the irreducible point group of the crystal for which they are constructed. This is a particularly useful property, because it leads to a block-diagonal matrix representation for the BE (8.7). For single sheet, cubic symmetry energy surfaces, the lowest order Fermi surface harmonics are $F_J(\boldsymbol{k}) = v_J(\boldsymbol{k})/v(E(\boldsymbol{k}))$ with $J = X, Y, Z$ and a normalization factor $v(E) = [N(E)^{-1} \sum_{\boldsymbol{k}} v_x(\boldsymbol{k})^2 \delta(E(\boldsymbol{k}) - E)]^{1/2}$, which is the root-mean-square velocity at the energy surface E. Further details about Fermi surface harmonics, in particular, the construction principle for arbitrary energy surfaces, can be found in [36].

The energy polynomials $\sigma_n(E)$ are n^{th} order polynomials in $E/(k_{\rm B}T)$, which are orthogonal with respect to the weight function $-\partial f/\partial E$ with

$$\int {\rm d}E \left(-\frac{\partial f}{\partial E}\right) \sigma_n(E)\sigma_{n'}(E) = \delta_{nn'} \ . \tag{8.34}$$

They will be used to describe variations perpendicular to the Fermi surface. The first two polynomials are $\sigma_0(E) = 1$ and $\sigma_1(E) = \sqrt{3}E/(\pi k_{\rm B}T)$. Higher order ones have to be again constructed on a computer, using the recursion relation given by Allen [37]. As pointed out by Pinski [38], another possible choice for the energy polynomials, which may lead to faster convergence in some cases, is $\sigma_n(E) = \sqrt{2n+1}P_n(\tanh[E/(2k_{\rm B}T)])$, where $P_n(E)$ is the $n^{\rm th}$ order Legendre polynomial.

Allen used the functions $F_J(\boldsymbol{k})$ and $\sigma_n(E(\boldsymbol{k}))$ to define two complete sets of functions which are biorthogonal. With the proper normalization, they are given by

$$\begin{aligned} \chi_{Jn}(\boldsymbol{k}) &= \frac{F_J(\boldsymbol{k})\sigma_n(E(\boldsymbol{k}))}{N(E(\boldsymbol{k}))v(E(\boldsymbol{k}))} \ , \\ \xi_{Jn}(\boldsymbol{k}) &= -F_J(\boldsymbol{k})\sigma_n(E(\boldsymbol{k}))v(E(\boldsymbol{k}))\frac{\partial f}{\partial E}\bigg|_{E(\boldsymbol{k})} \end{aligned} \tag{8.35}$$

with $N(E)$ and $v(E)$, respectively, the single-spin density of states and the root-mean-square velocity at energy E (see above). With the help of (8.33) and (8.34), it is straightforward to show that $\chi_{Jn}(\boldsymbol{k})$ and $\xi_{Jn}(\boldsymbol{k})$ satisfy the biorthogonality conditions

$$\begin{aligned} \sum_{\boldsymbol{k}} \chi_{Jn}(\boldsymbol{k})\xi_{J'n'}(\boldsymbol{k}) &= \delta_{JJ'}\delta_{nn'} \ , \\ \sum_{Jn} \chi_{Jn}(\boldsymbol{k})\xi_{Jn}(\boldsymbol{k}') &= \delta_{\boldsymbol{k}\boldsymbol{k}'} \ . \end{aligned} \tag{8.36}$$

Any function of $\boldsymbol{k}$ can be either expanded in terms of the functions $\chi_{Jn}(\boldsymbol{k})$ or in terms of the functions $\xi_{Jn}(\boldsymbol{k})$. The functions χ_{Jn} are most convenient for expanding functions which are smooth in energy. Since in (8.29) we split-off the factor $-\partial_E f$, we expect $\phi(\boldsymbol{k})$ to exhibit this property and thus write

$$\phi(\boldsymbol{k}) = \sum_{Jn} \phi_{Jn}\chi_{Jn}(\boldsymbol{k}) \ . \tag{8.37}$$

The functions ξ_{Jn}, on the other hand, vary strongly in the vicinity of the Fermi surface. They are used at intermediate steps to express functions which peak at the Fermi energy.

We are now able to rewrite (8.31). Using the definition of ξ_{Jn}, the l.h.s. immediately becomes

$$\text{l.h.s. of (8.31)} = eE_x\xi_{X0}(\boldsymbol{k}) \ . \tag{8.38}$$

For the r.h.s., we find

$$\begin{aligned}\text{r.h.s. of (8.31)} &= \sum_{\boldsymbol{k}'\boldsymbol{k}''} Q_{\boldsymbol{k}\boldsymbol{k}'}\delta_{\boldsymbol{k}'\boldsymbol{k}''}\phi(\boldsymbol{k}'') \\ &= \sum_{J'n'}\sum_{\boldsymbol{k}'} Q_{\boldsymbol{k}\boldsymbol{k}'}\chi_{J'n'}(\boldsymbol{k}')\sum_{\boldsymbol{k}''}\xi_{J'n'}(\boldsymbol{k}'')\phi(\boldsymbol{k}'') \\ &= \sum_{J'n'}\sum_{\boldsymbol{k}'} Q_{\boldsymbol{k}\boldsymbol{k}'}\chi_{J'n'}(\boldsymbol{k}')\phi_{J'n'} \ , \end{aligned} \tag{8.39}$$

where in the second line we expressed the Kronecker delta via (8.36) and in the third line we used the inverse of (8.37)

$$\phi_{Jn} = \sum_{\boldsymbol{k}} \xi_{Jn}(\boldsymbol{k})\phi(\boldsymbol{k}) \ . \tag{8.40}$$

Multiplying (8.38) and (8.39) from the left with $\chi_{Jn}(\boldsymbol{k})$ and summing over all $\boldsymbol{k}$ leads to the final result

$$E_x\delta_{n0}\delta_{JX} = \sum_{J'n'} Q_{Jn,J'n'}\phi_{J'n'} \tag{8.41}$$

with $Q_{Jn,J'n'} = \sum_{\boldsymbol{k}\boldsymbol{k}'} \chi_{Jn}(\boldsymbol{k})Q_{\boldsymbol{k}\boldsymbol{k}'}\chi_{J'n'}(\boldsymbol{k}')$.

Equation (8.41) is the symmetry-adapted matrix representation of the linearized BE (8.31). Its solution gives the expansion coefficients ϕ_{Jn}. To complete the calculation, we have to express the electric current j_x in terms of these coefficients. Using in (8.30) the definition for $\xi_{X0}(\boldsymbol{k})$ and the biorthogonality condition (8.36), we obtain

$$j_x = 2e\phi_{X0} \ , \tag{8.42}$$

which with (8.41) yields

$$\sigma_{xx} = 2e^2[Q^{-1}]_{X0,X0} \ . \tag{8.43}$$

Thus, in Allen's basis, the xx-component of the electric conductivity tensor is just the upper-most left matrix element of the inverse of the matrix which represents the linearized collision integral. Remember, because of the symmetry of the basis functions, this matrix is block-diagonal. The numerical inversion is therefore expected to be fast.

The numerical bottleneck is the calculation of the matrix elements $Q_{Jn,J'n'}$. They depend on the symmetry of the metal and, of course, on the scattering processes. For realistic band structures, this leads to rather involved expressions, which, fortunately, are amenable to some simplifications arising from the fact that in metals $k_{\mathrm{B}}T/E_F \ll 1$, where E_F is the Fermi energy. The $\boldsymbol{k}$-integration can thus be restricted to the thermal layer with width Δk, see Fig. 8.3. For explicit expressions, we refer to the literature [37, 38, 39, 40, 41, 42, 43]. Although Allen's approach is not straightforward to implement, it has the advantage that it can handle complicated Fermi surfaces in a transparent manner. In practice, the matrix elements $Q_{Jn,J'n'}$ are expressed in terms of generalized coupling functions which can be either directly obtained from experiments or from ab initio band structure calculations. Allen's method of solving the linearized BE is therefore geared towards an ab initio calculation of transport coefficients for metals.

8.2.3 Particle-Based Monte Carlo Simulation

The most widely accepted method for solving the electron transport problem in semiconductors is the particle-based Monte Carlo simulation [44, 45, 46, 47, 48, 49]. In its general form, it simulates the stochastic motion of a finite number of test-particles and is equivalent to the solution of the BE. This technique has been, for instance, used to simulate field-effect transistors from a microscopic point of view, starting from the band structures and scattering processes of the semiconducting materials transistors are made off.

A Monte Carlo simulation of Boltzmann transport is a one-to-one realization of Boltzmann's original idea of free flights, occasionally interrupted by random scattering events, as being responsible for the macroscopic transport properties of the gas under consideration; here, the electrons in a semiconductor. The approach relies only on general concepts of probability theory, and not on specialized mathematical techniques. Because of the minimum of mathematical analysis, realistic band structures, scattering probabilities, and geometries can be straightforwardly incorporated into a Monte Carlo code. However, the method has some problems to account for Pauli-blocking in degenerate electron systems. It has thus not been applied to degenerate semiconductors, metals, or quantum fluids.

8.2.3.1 Spatially Uniform, Steady-State BE with the Full Collision Integral

First, we focus on the simplest situation: Steady-state transport in a spatially uniform, non-degenerate semiconductor. For the techniques described in the previous Subsections, this situation is already rather demanding, in particular, when a realistic electronic structure is used, which leads to involved $\boldsymbol{k}$-summations. The Monte Carlo simulation, on the other hand, requires no $\boldsymbol{k}$-summations. Moreover, in that particular case, transport coefficients for electrons can be calculated rather easily because ergodicity guarantees that the simulation of a single test-particle is sufficient to sample the whole phase space.

Instead of attempting to solve

$$\left\{-\frac{e}{\hbar}\boldsymbol{E}\cdot\nabla_{\boldsymbol{k}}+\lambda_{\boldsymbol{k}}+S_{\boldsymbol{k}}\right\}\, g(\boldsymbol{k},t)=\sum_{\boldsymbol{k}'}\left[S_{\boldsymbol{k}',\boldsymbol{k}}+S_{\boldsymbol{k}}\delta_{\boldsymbol{k}\boldsymbol{k}'}\right]\, g(\boldsymbol{k}',t)\;, \tag{8.44}$$

which is the BE appropriate for steady-state transport in a single band of a semiconductor subject to an uniform electric field, the Monte Carlo approach simulates the motion of a single test-electron in momentum space. For that purpose, it generates a large number of free flights, where the test-electron drifts freely in the electric field until it suffers one of the possible scattering processes, see Fig. 8.4. The technique uses random variables to represent the duration of the free flight, to select the type of scattering which terminates the free flight, and to determine the momentum of the test-electron after the scattering event, which is then used as the initial momentum for the next free flight. The steady-state does not depend on the initial condition for the first free flight. Any convenient choice can therefore be made.

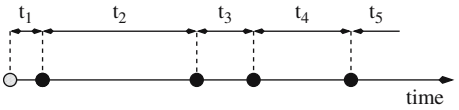

Fig. 8.4. Schematic representation of the particle-based Monte Carlo simulation of steady-state Boltzmann transport in spatially uniform solids. A single test-particle suffices here because ergodicity guarantees that the whole phase space is sampled. The test-particle performs free flights in the external field, randomly interrupted by one of the possible scattering processes (*black bullets*). The simulation consists of a finite number of free flights, starting from an arbitrary initial condition (*grey bullet*). For each free flight the simulation uses random numbers to generate its duration t_i, to select the terminating scattering process, and to determine the test-particles' momentum after the scattering event, which then serves as the initial momentum for the next free flight

Because of ergodicity, the ensemble average of a single-particle observable $O(\boldsymbol{k})$ is equal to the time average of this observable. Splitting the total simulation time t_s into a finite number of free flights with duration t_i we obtain

$$\langle O\rangle = \langle O\rangle_{t_s} = \sum_i \frac{1}{t_s}\int_0^{t_i} \mathrm{d}t\; O(\boldsymbol{k}(t))\;, \tag{8.45}$$

where O can be, for instance, the energy of the electron $E(\boldsymbol{k})$ or its velocity $\boldsymbol{v}(\boldsymbol{k}) = \hbar^{-1}\nabla_{\boldsymbol{k}}E(\boldsymbol{k})$. Note, for each free flight, the time integration starts all over again from zero. The test-electron has no memory, reminiscent of the Markovian property of the BE.

The probability distributions for the random variables used in the Monte Carlo simulation are given in terms of the electric field and the transition probabilities for the various scattering processes. For realistic band structures the distributions can be quite complicated, in particular, the distribution of the duration of the free flights. Special techniques have to be used to relate the random variables needed in the simulation to the uniformly distributed random variables generated by a computer.

Let us first consider the distribution of the duration of the free flights. The probability for the test-electron to suffer the next collision in the time interval $\mathrm{d}t$ centered around t is given by

$$P(t)\mathrm{d}t = \widetilde{\lambda}_{\boldsymbol{k}(t)}\mathrm{e}^{-\int_0^t \mathrm{d}t'\widetilde{\lambda}_{\boldsymbol{k}(t')}}\mathrm{d}t\;, \tag{8.46}$$

where $\boldsymbol{k}(t) = \boldsymbol{k}_0 - (e/\hbar)\boldsymbol{E}t$, with $\boldsymbol{k}_0$ the arbitrary wave vector from which the first free flight started, and $\widetilde{\lambda}_{\boldsymbol{k}}$ the total transition rate from state $\boldsymbol{k}$ due to all scattering processes, including selfscattering. In Sect. 8.2.1, we introduced selfscattering in order to simplify the integral representation of the BE. But it is also very useful in the present context because, using again the choice (8.26), it leads to $\widetilde{\lambda} = \Gamma$ and thus to

$$P(t)\mathrm{d}t = \Gamma\mathrm{e}^{-\Gamma t}\mathrm{d}t\,. \tag{8.47}$$

Note, without selfscattering, we should have integrated over $\lambda_{\boldsymbol{k}(t)}$, comprising only real scattering events. For realistic band structures, this could have been done only numerically, and would have lead to a rather complicated $P(t)\mathrm{d}t$, useless for further numerical processing.

To relate the random variable t to a random variable $R \in [0,1]$ with a uniform distribution, we consider the cumulant of $P(t)$,

$$c(t) = \int_0^t \mathrm{d}t' P(t') = 1 - \mathrm{e}^{-\Gamma t} \; , \tag{8.48}$$

which for a random value of t is a random variable R, uniformly distributed between $[0,1]$ because $c(0) = 0$ and $c(\infty) = 1$. Thus, $c(t) = R$. Inverting (8.48) and introducing a new random variable $R_1 = 1 - R$, which is also uniformly distributed in $[0,1]$, the duration of the free flights can be easily generated by

$$t = -\frac{1}{\Gamma} \ln R_1 \; . \tag{8.49}$$

Having determined the duration of a free flight, a scattering event, responsible for the end of the free flight, has to be chosen. As mentioned before, we assume that $\widetilde{\lambda}_{\boldsymbol{k}}$ is the total transition rate from state $\boldsymbol{k}$, which is now the terminating momentum of the free flight, including selfscattering, that is, $\widetilde{\lambda}_{\boldsymbol{k}} = \sum_{p=1}^{N} \lambda_{\boldsymbol{k}}^p + S_{\boldsymbol{k}} = \sum_{p=1}^{N+1} \lambda_{\boldsymbol{k}}^p$, where N is the total number of real scattering processes and $\lambda_{\boldsymbol{k}}^{N+1} = S_{\boldsymbol{k}}$. From definition (8.26) follows $\widetilde{\lambda}_{\boldsymbol{k}} = \Gamma$. One way of choosing the terminating scattering process is therefore to generate a random variable $R_2 \in [0,1]$ and to form partial sums until

$$\frac{1}{\Gamma} \sum_{p=1}^{m-1} \lambda_{\boldsymbol{k}}^p < R_2 \leq \frac{1}{\Gamma} \sum_{p=1}^{m} \lambda_{\boldsymbol{k}}^p \tag{8.50}$$

is satisfied. The m^{th} process is then the terminating one.

Equation (8.50) contains selfscattering and real scattering processes. In the former the momentum is conserved, that is, $\boldsymbol{k} = \boldsymbol{k}'$, with $\boldsymbol{k}'$ the momentum after the scattering event. For real scattering processes, however, $\boldsymbol{k}'$ is a random variable which has to be determined from the transition probabilities of the various scattering processes whose precise forms in turn depend on the material. We describe therefore only the basic strategy for choosing the momentum of the test-electron after the scattering event, assuming electron-impurity and electron-phonon scattering to be responsible for the end of the free flight, see Fig. 8.5.

From the momentum $\boldsymbol{k}$ the test-electron has at the end of the free flight, we obtain its energy $E(\boldsymbol{k})$ before the scattering event. Energy conservation can then be used to determine the energy E' of the test-electron after the scattering event. For electron-impurity scattering $E' = E(\boldsymbol{k})$ (elastic scattering) whereas for electron-phonon scattering $E' = E(\boldsymbol{k}) \pm \hbar\omega$, where for simplicity we assumed dispersionless phonons with energy $\hbar\omega$. The upper and lower sign corresponds, respectively, to phonon absorption and emission, which are treated here as separate processes. In most cases, the part of the semiconductors' band structure relevant for transport can

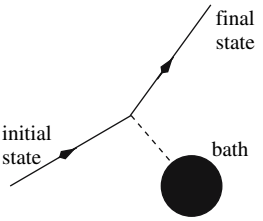

Fig. 8.5. Illustration of the scattering event in the test-particle-based Monte Carlo simulation. The test-particle scatters off a generalized bath representing impurities and phonons. For elastic scattering, the test-electron gains or loses only momentum, whereas for inelastic scattering it can also transfer or receive energy

be assumed to be isotropic. The magnitude of the final state momentum, $k' = |\boldsymbol{k}'|$ can thus be obtained from $E' = E(k')$. The orientation of the vector $\boldsymbol{k}'$, however, is still unspecified.

When the scattering process is randomizing, all momentum states on the final state energy surface are equally probable. Measuring the orientation of $\boldsymbol{k}'$ in polar coordinates, with $\boldsymbol{k}$ pointing in the z-direction, the probability[12] for $\boldsymbol{k}'$ to be given by $k'_x = k' \cos\phi' \sin\theta'$, $k'_y = k' \sin\phi' \sin\theta'$, and $k'_z = k' \cos\theta'$, with $0 \leq \phi' \leq 2\pi$ and $0 \leq \theta' \leq \pi$, is $P(\phi', \theta') = (1/4\pi) \sin\theta'$. To relate the random variables ϕ' and θ' to two uniformly distributed random variables in the interval $[0, 1]$, we first condition the two-variable probability $P(\phi', \theta')$ in the form

$$P(\phi', \theta') = P_1(\phi') P_2(\theta'|\phi') \; , \tag{8.51}$$

where $P_1(\phi') = \int_0^\pi \mathrm{d}\theta' P(\phi', \theta') = 1/(2\pi)$ is the marginal probability for ϕ' and $P_2(\theta'|\phi') = P(\phi', \theta')/(P_1(\phi')) = \sin\theta'/2$ is the conditional probability for θ' given ϕ'. We then apply cumulants (as described above) separately to P_1 and P_2 and obtain

$$\begin{aligned} \phi' &= 2\pi R_3 \; , \\ \cos\theta' &= 1 - 2R_4 \end{aligned} \tag{8.52}$$

with R_3 and R_4 uniformly distributed random variables in the interval $[0, 1]$.

For non-randomizing scattering processes, the probability for the angles is proportional to the transition rate written in the polar coordinates introduced above. Hence, for given k and k', the properly normalized function $P(\phi', \theta'; k, k') = (\sin\theta'/4\pi) S(k, k', \phi', \theta')$ gives the probability for the azimuth ϕ' and the polar angle θ', both depending therefore on k and k'. Applying again the method of conditioning, which can be applied to any two-variable probability, together with the cumulants, the random variables $\phi'(k, k')$ and $\theta'(k, k')$ can be again expressed in terms of uniformly distributed random variables in the interval $[0, 1]$.

The simulation consists of a finite number of free flights of random duration and random initial conditions. Average single particle properties, in particular the

[12] Strictly speaking, it is the probability density.

drift velocity, can then be obtained from (8.45). Assuming the electric field to be in z-direction, the drift will be also along the z-axis, that is, only the z-component of the electron momentum will be changed due to the field. Hence, writing (8.45) with $O = v_z(k_z(t))$ and integrating with respect to k_z instead of t, the drift velocity is given by [44]

$$\langle v_z \rangle = \frac{1}{K} \sum_{\text{flights}} \int_{k_{z,i}}^{k_{z,f}} \frac{1}{\hbar} \frac{\partial E}{\partial k_z} \, \mathrm{d}k_z = \frac{1}{\hbar K} \sum_{\text{flights}} (E_f - E_i) \, , \tag{8.53}$$

where the sum goes over all free flights, $k_{z,i}$ and $k_{z,f}$ denote the z-component of the initial and final momentum of the respective free flights, and K is the total length of the $\boldsymbol{k}$-space trajectory.

In some cases, the distribution function $g(\boldsymbol{k})$ may be also of interest. In order to determine $g(\boldsymbol{k})$ from the motion of a single test-particle a grid is set up in momentum space at the beginning of the simulation. During the simulation the fraction of the total time the test-electron spends in each cell is then recorded and taken as a measure for the distribution function. This rule results from an application of (8.45). Indeed, using $O(\boldsymbol{k}(t)) = n_i(\boldsymbol{k}(t))$ with $n_i(\boldsymbol{k}(t)) = 1$ when the test-particle is in cell i and zero otherwise, gives $g(\boldsymbol{k}_i) \equiv \langle n_i \rangle = \Delta t_i / t_s$, with Δt_i the time spend in cell i. Averaged single particle quantities for the steady-state could then be also obtained from the sum

$$\langle O \rangle = \sum_{\boldsymbol{k}} O(\boldsymbol{k}) g(\boldsymbol{k}) \, , \tag{8.54}$$

but for a reasonable accuracy the grid in momentum space has to be very fine. It is therefore more convenient to calculate $\langle O \rangle$ directly from (8.45).

It is instructive to demonstrate that the Monte Carlo procedure just outlined is indeed equivalent to solving the steady-state BE (8.44). The equivalence proof has been given by Fawcett and coauthors [44] and we follow closely their treatment. The starting point is the definition of a function $P_n(\boldsymbol{k}_0, \boldsymbol{k}, t)$ which is the probability that the test-electron will have momentum $\boldsymbol{k}$ at time t during the n^{th} free flight when it started at $t = 0$ with momentum $\boldsymbol{k}_0$. The explicit time dependence must be retained because the electron can pass through the momentum state $\boldsymbol{k}$ any time during the n^{th} free flight. This probability satisfies an integral equation

$$\begin{aligned} P_n(\boldsymbol{k}_0, \boldsymbol{k}, t) = \sum_{\boldsymbol{k}', \boldsymbol{k}''} \int_0^t \mathrm{d}t' P_{n-1}(\boldsymbol{k}_0, \boldsymbol{k}', t) \widetilde{S}_{\boldsymbol{k}', \boldsymbol{k}''} \\ \times \mathrm{e}^{-\int_0^{t-t'} \mathrm{d}t'' \widetilde{\boldsymbol{\lambda}}_{\boldsymbol{k}'' - e\boldsymbol{E}t''/\hbar}} \delta_{\boldsymbol{k}, \boldsymbol{k}'' - e\boldsymbol{E}(t-t')/\hbar} \, , \end{aligned} \tag{8.55}$$

whose r.h.s. consists of three probabilities which are integrated over. The first one $P_{n-1}(\boldsymbol{k}_0, \boldsymbol{k}', t)$ is the probability that the test-electron passes through some momentum state $\boldsymbol{k}'$ during the $(n-1)^{th}$ free flight, the second $\widetilde{S}_{\boldsymbol{k}', \boldsymbol{k}''}$ is the probability that it will be scattered from state $\boldsymbol{k}'$ to state $\boldsymbol{k}''$, whereas the exponential factor

is the probability that it will not be scattered while drifting from $\boldsymbol{k}''$ to $\boldsymbol{k}$ during the n^{th} free flight. The Kronecker-δ ensures that the test-electron follows the trajectory appropriate for the applied electric field $\boldsymbol{E}$. The Monte Carlo simulation generates realizations of the random variable $\boldsymbol{k}(t)$ in accordance to the probability $P_n(\boldsymbol{k}_0, \boldsymbol{k}, t)$.

Integrating in (8.55) over $\boldsymbol{k}''$ and t' and substituting $\tau = t - t'$ and $y = \tau - t''$ yields an equation,

$$P_n(\boldsymbol{k}_0, \boldsymbol{k}, t) = \sum_{\boldsymbol{k}'} \int_0^t \mathrm{d}\tau P_{n-1}(\boldsymbol{k}_0, \boldsymbol{k}', t-\tau) \widetilde{S}_{\boldsymbol{k}', \boldsymbol{k}+e\boldsymbol{E}\tau/\hbar} \, \mathrm{e}^{-\int_0^\tau \mathrm{d}y \widetilde{\boldsymbol{\lambda}}_{\boldsymbol{k}+e\boldsymbol{E}y/\hbar}} \, , \tag{8.56}$$

which is a disguised BE. To make the connection with the BE more explicit, we consider the count at $\boldsymbol{k}$ obtained after N collisions

$$C_N(\boldsymbol{k}_0, \boldsymbol{k}) = \lim_{t_s \to \infty} \sum_{n=1}^{N} \frac{1}{t_s} \int_0^{t_s} \mathrm{d}t P_n(\boldsymbol{k}_0, \boldsymbol{k}, t) \, . \tag{8.57}$$

This number is provided by the Monte Carlo procedure and at the same time it can be identified with $g(\boldsymbol{k})$ for $N \gg 1$. Thus, $C_N(\boldsymbol{k}_0, \boldsymbol{k})$ is the bridge, which will carry us from the test-particle Monte Carlo simulation to the traditional BE.

We now perform a series of mathematical manipulations at the end of which we will have obtained the steady-state, spatially-uniform BE (8.44). Inserting (8.56) into the definition (8.57), applying on both sides $-(e/\hbar)\boldsymbol{E} \cdot \nabla_{\boldsymbol{k}}$ from the left, and using the two identities

$$\begin{aligned} -\frac{e\boldsymbol{E}}{\hbar} \cdot \nabla_{\boldsymbol{k}} \widetilde{S}_{\boldsymbol{k}', \boldsymbol{k}+e\boldsymbol{E}\tau/\hbar} &= -\frac{\partial}{\partial \tau} \widetilde{S}_{\boldsymbol{k}', \boldsymbol{k}+e\boldsymbol{E}\tau/\hbar} \, , \\ -\frac{e\boldsymbol{E}}{\hbar} \cdot \nabla_{\boldsymbol{k}} \mathrm{e}^{-\int_0^\tau \mathrm{d}y \widetilde{\boldsymbol{\lambda}}_{\boldsymbol{k}+e\boldsymbol{E}y/\hbar}} &= -\left(\frac{\partial}{\partial \tau} + \widetilde{\lambda}_{\boldsymbol{k}} \right) \mathrm{e}^{-\int_0^\tau \mathrm{d}y' \widetilde{\boldsymbol{\lambda}}_{\boldsymbol{k}+e\boldsymbol{E}y/\hbar}} \end{aligned} \tag{8.58}$$

gives

$$-\frac{e\boldsymbol{E}}{\hbar} \cdot \nabla_{\boldsymbol{k}} C_N(\boldsymbol{k}_0, \boldsymbol{k}) = -\widetilde{\lambda}_{\boldsymbol{k}} C_N(\boldsymbol{k}_0, \boldsymbol{k})$$

$$- \lim_{t_s \to \infty} \sum_{n=1}^{N} \frac{1}{t_s} \sum_{\boldsymbol{k}'} \int_0^{t_s} \mathrm{d}\tau P_{n-1}(\boldsymbol{k}_0, \boldsymbol{k}', t-\tau) \frac{\partial}{\partial \tau} \left[\widetilde{S}_{\boldsymbol{k}', \boldsymbol{k}+e\boldsymbol{E}\tau/\hbar} \mathrm{e}^{-\int_0^\tau \mathrm{d}y \widetilde{\boldsymbol{\lambda}}_{\boldsymbol{k}+e\boldsymbol{E}y/\hbar}} \right] , \tag{8.59}$$

where we used definition (8.57) once more to obtain the first term on the r.h.s. This equation can be rewritten into

$$
\begin{aligned}
-\frac{e\boldsymbol{E}}{\hbar}\cdot\nabla_{\boldsymbol{k}}C_N(\boldsymbol{k}_0,\boldsymbol{k}) &= -\widetilde{\lambda}_{\boldsymbol{k}}C_N(\boldsymbol{k}_0,\boldsymbol{k}) \\
&- \lim_{t_s\to\infty}\sum_{n=1}^{N}\frac{1}{t_s}\int_0^{t_s}\mathrm{d}t\sum_{\boldsymbol{k}'}P_{n-1}(\boldsymbol{k}_0,\boldsymbol{k}',0)\widetilde{S}_{\boldsymbol{k}',\boldsymbol{k}+e\boldsymbol{E}t/\hbar}\mathrm{e}^{-\int_0^t\mathrm{d}y\widetilde{\boldsymbol{\lambda}}_{\boldsymbol{k}+e\boldsymbol{E}y/\hbar}} \\
&+ \lim_{t_s\to\infty}\sum_{n=1}^{N}\frac{1}{t_s}\int_0^{t_s}\mathrm{d}t\sum_{\boldsymbol{k}'}P_{n-1}(\boldsymbol{k}_0,\boldsymbol{k}',t)\widetilde{S}_{\boldsymbol{k}',\boldsymbol{k}} - \lim_{t_s\to\infty}\sum_{n=1}^{N}\frac{1}{t_s}\int_0^{t_s}\mathrm{d}t \\
&\times\sum_{\boldsymbol{k}'}\int_0^{t}\mathrm{d}\tau\frac{\partial}{\partial t}\left(P_{n-1}(\boldsymbol{k}_0,\boldsymbol{k}',t-\tau)\widetilde{S}_{\boldsymbol{k}',\boldsymbol{k}+e\boldsymbol{E}\tau/\hbar}\mathrm{e}^{-\int_0^\tau\mathrm{d}y\widetilde{\boldsymbol{\lambda}}_{\boldsymbol{k}+e\boldsymbol{E}y/\hbar}}\right)\,, \qquad (8.60)
\end{aligned}
$$

when the τ-integration is carried out by parts and $\partial_\tau P_{n-1} = -\partial_t P_{n-1}$ is used. Pulling now in the fourth term on the r.h.s. the differential operator ∂_t in front of the τ-integral produces two terms, one of which cancels with the second term on the r.h.s. and the other vanishes in the limit $t_s \to \infty$. As a result, only the first and third term on the r.h.s. of (8.60) remain. Using finally in the third term again the definition (8.57) yields

$$
-\frac{e\boldsymbol{E}}{\hbar}\cdot\nabla_{\boldsymbol{k}}C_N(\boldsymbol{k}_0,\boldsymbol{k}) + \widetilde{\lambda}_{\boldsymbol{k}}C_N(\boldsymbol{k}_0,\boldsymbol{k}) = \sum_{\boldsymbol{k}'}C_{N-1}(\boldsymbol{k}_0,\boldsymbol{k}')\widetilde{S}_{\boldsymbol{k}',\boldsymbol{k}}\,, \qquad (8.61)
$$

which, recalling the definitions of $\widetilde{\lambda}_{\boldsymbol{k}}$ and $\widetilde{S}_{\boldsymbol{k}',\boldsymbol{k}}$ and using $C_{N-1}(\boldsymbol{k}_0,\boldsymbol{k}) \to C_N(\boldsymbol{k}_0, \boldsymbol{k}) \to g(\boldsymbol{k})$ for $N \to \infty$, is identical to the BE (8.44). Thus, the simulation of a large number of free flights, each one terminating in a random scattering event, indeed simulates the steady-state BE for a spatially uniform semiconductor.

8.2.3.2 Spatially Non-Uniform BE with the Full Collision Integral

For spatially non-uniform situations[13], typical for semiconductor devices, the simulation of a single test-particle is not enough (see Fig. 8.6). With a single test-particle, for instance, it is impossible to represent the source term of the Poisson equation. However, this equation needs to be solved in conjunction with the BE to obtain the self-consistent electric field responsible for space-charge effects which, in turn, determine the current-voltage characteristics of electronic devices.

Instead of a single test particle it is necessary to simulate an ensemble of test-particles for prescribed boundary conditions for the Poisson equation and the BE, where the latter have to be translated into boundary conditions for the test-particles. The boundary conditions for the Poisson equation are straightforward; Dirichlet condition, i.e., fixed potentials, at the electrodes and Neumann condition, i.e., zero electric field, at the remaining boundaries. But the boundary conditions for the test-particles, which need to be consistent with the ones for the Poisson equation, can be rather subtle, resulting in sophisticated particle injection and reflection strategies,

[13] The same holds for time-dependent situations.

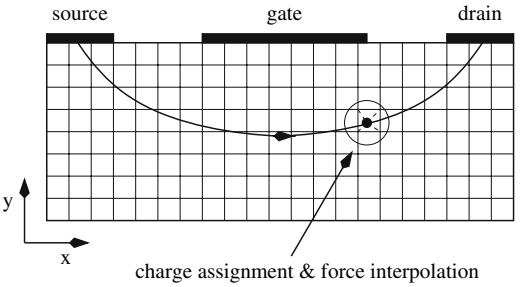

Fig. 8.6. Schematic representation of the cross section of a metal-semiconductor field-effect transistor (MESFET). Shown is a typical discretization of the two-dimensional simulation volume, a representative electron trajectory, and the contacting through a source, a gate, and a drain electrode. The BE has to be solved together with the Poisson equation; for both equations boundary conditions are required, see Sect. 8.2.3.2. Since the Poisson equation is grid-bound, whereas the BE is not, charge assignment and force interpolation symbolized by the thin lines inside the circle are required for the simultaneous solution of the two

in particular, when the doping profile of the semiconductor structure is taken into account. An authoritative discussion of the boundary conditions, as well as other aspects of device modeling, can be found in the textbook by Jacoboni and Lugli [47].

Conceptually, the Monte Carlo simulation for semiconductor devices resembles the particle-in-cell simulations for plasmas described in Chap. 6, and we refer there for technical details. In particular, the techniques for the solution of the Poisson equation and the particle weighting and force interpolation required for the coupling of the grid-free electron kinetics (simulation of the BE) with the grid-bound electric field (solution of the Poisson equation) are identical. In addition, except of the differences which arise from the particular electric contacting of the simulation volume, the implementation of particle injection and reflection (boundary conditions for the test-particles) are also basically the same. The only differences are that the test-particles have to be of course propagated during a free flight according to $\mathrm{d}\boldsymbol{k}/\mathrm{d}t = -(e/\hbar)\boldsymbol{E}$ and $\mathrm{d}\boldsymbol{r}/\mathrm{d}t = \hbar^{-1}\nabla_{\boldsymbol{k}}E(\boldsymbol{k})$ and that the scattering processes are the ones appropriate for semiconductors: Electron-impurity scattering, electron-phonon scattering, and, in some cases, electron-electron scattering.

In this generalized form, the particle-based Monte Carlo simulation has become the standard tool for analyzing Boltzmann transport of electrons in semiconductors. In combination with ab initio band structure data, including scattering rates, it is by now an indispensable tool for electronics engineers optimizing the performance of semiconductor devices [46, 47, 48, 49].

8.2.4 Ensemble-Based Monte Carlo Simulation

The test-particle-based Monte Carlo algorithm described in the previous Subsection cannot be applied to degenerate electron systems where the final state of the scattering may be blocked by the Pauli principle. Mathematically, the Pauli-blocking is

encoded in the collision integral (8.6) through the factor $1 - g_n(\boldsymbol{r}, \boldsymbol{k}, t)$. It depends therefore on the one-particle distribution function which in the test-particle-based Monte Carlo algorithm is only available at the end of the simulation. In principle, the distribution function from a previous run could be used, but this requires additional book-keeping, which, if nothing else, demonstrates that the algorithm presented in the previous Subsection loses much of its simplicity.

An alternative method, which is most suitable for degenerate Fermi systems is the ensemble-based Monte Carlo simulation. There are various ways to simulate an ensemble. We describe here a simple approach, applicable to a spatially homogeneous electron system. It is based on the master equation for the probability $P_\nu(t)$ that at time t the many-particle system is in configuration $\nu = (n_{\boldsymbol{k}_1}, n_{\boldsymbol{k}_2}, ...)$. For fermions, $n_{\boldsymbol{k}_i} = 0$ when the momentum state $\boldsymbol{k}_i$ is empty and $n_{\boldsymbol{k}_i} = 1$ when the state is occupied. The one-particle distribution function, which is the solution of the corresponding BE, is then given by an ensemble average

$$g(\boldsymbol{k}, t) = \sum_\nu P_\nu(t) n_{\boldsymbol{k}} \; . \tag{8.62}$$

The algorithm has been developed by El-Sayed and coworkers and we closely follow their treatment [50]. The purpose of the algorithm is to simulate electron relaxation in a two-dimensional, homogeneous degenerate electron gas, with electron-electron scattering as the only scattering process. Such a situation can be realized, for instance, in the conduction band of a highly optically excited semiconductor quantum well at low enough temperatures. It is straightforward to take other scattering processes into account. Inhomogeneous situations, typical for device modeling, can be in principle also treated but it requires a major overhaul of the approach which we will not discuss.

Taking only direct electron-electron scattering into account, the force-free Boltzmann equation for a homogeneous, two-dimensional electron gas reads[14]

$$\frac{\partial g_{\boldsymbol{k}}}{\partial t} = 2 \sum_{\boldsymbol{p},\boldsymbol{k}'\boldsymbol{p}'} W_{\boldsymbol{k}\boldsymbol{p};\boldsymbol{k}'\boldsymbol{p}'} \left([1 - g_{\boldsymbol{k}}][1 - g_{\boldsymbol{p}}] g_{\boldsymbol{k}'} g_{\boldsymbol{p}'} - g_{\boldsymbol{k}} g_{\boldsymbol{p}} [1 - g_{\boldsymbol{k}'}][1 - g_{\boldsymbol{p}'}] \right) \tag{8.63}$$

with

$$W_{\boldsymbol{k}\boldsymbol{p};\boldsymbol{k}'\boldsymbol{p}'} = \frac{2\pi}{\hbar} \left| V(|\boldsymbol{k} - \boldsymbol{k}'|) \right|^2 \delta_{\boldsymbol{k}+\boldsymbol{p};\boldsymbol{k}'+\boldsymbol{p}'} \delta \left(E(\boldsymbol{k}) + E(\boldsymbol{p}) - E(\boldsymbol{k}') - E(\boldsymbol{p}') \right) \tag{8.64}$$

and $V(q) = 2\pi e^2/[\epsilon_0(q + q_s)]$ the statically screened Coulomb interaction in two dimensions, $V = L^2$ is again put to one. The factor two in front of the sum in (8.63) comes from the electron spin. As indicated above, the simulation of this equation via the test-particle-based Monte Carlo technique is complicated because the Pauli blocking factors depend on the (instantaneous) distribution function. The ensemble Monte Carlo method proposed by El-Sayed and coworkers [50] simulates therefore

[14] Notice the slight change in our notation: $g(\boldsymbol{k}) \to g_{\boldsymbol{k}}$.

the master equation underlying the Boltzmann description. This equation determines the time evolution of the probability for the occurrence of a whole configuration in momentum space,

$$\frac{\mathrm{d}P_\nu}{\mathrm{d}t} = -\frac{P_\nu(t)}{\tau_\nu} + \sum_{\nu'} W_{\nu'\nu} P_{\nu'}(t) \; . \tag{8.65}$$

Here

$$\frac{1}{\tau_\nu} = \sum_{\nu'} W_{\nu\nu'} \tag{8.66}$$

is the lifetime of the configuration ν, and $W_{\nu,\nu'}$ is the transition rate from configuration ν to ν'. Specifically for electron-electron scattering,

$$W_{\nu\nu'} = \frac{1}{2} \sum_{\boldsymbol{k}\boldsymbol{p}\boldsymbol{k}'\boldsymbol{p}'} W_{\boldsymbol{k}\boldsymbol{p};\boldsymbol{k}'\boldsymbol{p}'} n_{\boldsymbol{k}} n_{\boldsymbol{p}} [1 - n_{\boldsymbol{k}'}][1 - n_{\boldsymbol{p}'}] D^{\nu\nu'}_{\boldsymbol{k}\boldsymbol{p};\boldsymbol{k}'\boldsymbol{p}'} \tag{8.67}$$

with $D^{\nu\nu'}_{\boldsymbol{k}\boldsymbol{p};\boldsymbol{k}'\boldsymbol{p}'} = \delta_{n'_{\boldsymbol{k}} n_{\boldsymbol{k}} - 1} \delta_{n'_{\boldsymbol{p}} n_{\boldsymbol{p}} - 1} \delta_{n'_{\boldsymbol{k}'} n_{\boldsymbol{k}'} + 1} \delta_{n'_{\boldsymbol{p}'} n_{\boldsymbol{p}'} + 1} \prod_{\boldsymbol{q} \neq \boldsymbol{k},\boldsymbol{p},\boldsymbol{k}',\boldsymbol{p}'} \delta_{n'_{\boldsymbol{q}} n_{\boldsymbol{q}}}$.

The crucial point of the method is that the sampling of the configurations can be done in discrete time steps τ_ν. The master equation (8.65) then simplifies to

$$P_\nu(t + \tau_\nu) = \sum_{\nu'} \Pi_{\nu'\nu} P_{\nu'}(t) \tag{8.68}$$

with

$$\Pi_{\nu'\nu} = \tau_\nu W_{\nu'\nu} \tag{8.69}$$

the transition probability from configuration ν to configuration ν'[15]. Thus, when the system was at time t in the configuration ν_0, that is $P_\nu(t) = \delta_{\nu\nu_0}$, then the probability to find the system at time $t + \tau_\nu$ in the configuration ν is $P_\nu(t + \tau_\nu) = \Pi_{\nu_0\nu}$. In a simulation the new configuration can be therefore chosen according to the probability $\Pi_{\nu_0\nu}$.

However, there is a main drawback. In order to determine τ_ν form (8.66) a high-dimensional, configuration-dependent integral has to be numerically calculated before the time propagation can be made. Clearly, this is not very efficient. To overcome the problem, the selfscattering method is used again, but now at the level of the master equation, where selfscattering events can be also easily introduced because (8.65) is unchanged, when a diagonal element is added to the transition rate. It is therefore possible to work with a modified transition rate

$$W^s_{\nu\nu'} = W_{\nu\nu'} + W_\nu \delta_{\nu\nu'} \; , \tag{8.70}$$

giving rise to (cp. with (8.66))

[15] The normalization required for the interpretation of $\Pi_{\nu'\nu}$ in terms of a probability is a consequence of the detailed balance $W_{\nu\nu'} = W_{\nu'\nu}$ which holds for energy conserving processes.

$$\frac{1}{\tau_\nu^s} = \frac{1}{\tau_\nu} + W_\nu \; . \tag{8.71}$$

The diagonal elements of the modified transition probability $\Pi^s_{\nu_0\nu}$, that is, (8.69) with $\tau_\nu \to \tau_\nu^s$ and $W_{\nu_0\nu} \to W^s_{\nu_0\nu}$, are now finite. There is thus a finite probability to find the system at time $t + \tau_\nu^s$ still in the configuration ν_0, in other words, there is a finite probability for selfscattering $\nu \to \nu$.

Allowing for selfscattering provides us with the flexibility we need to speed up the simulation. Imagine τ_ν has a lower bound τ^s. Then, we can always add

$$W_\nu = \frac{1}{\tau^s} - \frac{1}{\tau_\nu} > 0 \tag{8.72}$$

to the transition rate which, when inserted in (8.71), leads to $\tau_\nu^s = \tau^s$. The sampling time step can be therefore chosen configuration independent, before the sampling starts. In addition, from the fact that τ^s is a lower bound to τ_ν follows $1/\tau_\nu \leq 1/\tau^s$. Thus, $1/\tau^s$ can be easily obtained from (8.66) using an approximate integrand which obeys or even enforces this inequality. In particular, using

$$n_{\boldsymbol{k}} n_{\boldsymbol{p}} \leq n_{\boldsymbol{k}} n_{\boldsymbol{p}} [1 - n_{\boldsymbol{k}'}][1 - n_{\boldsymbol{p}'}] \tag{8.73}$$

in (8.66) leads to

$$\frac{1}{\tau^s} = \frac{\gamma}{2} N(N-1) \; , \tag{8.74}$$

where $N = \sum_{\boldsymbol{k}} n_{\boldsymbol{k}}$ is the total number of electrons and $\gamma = \sup_{\boldsymbol{k},\boldsymbol{p}} \gamma_{\boldsymbol{k}\boldsymbol{p}}$ with $\gamma_{\boldsymbol{k}\boldsymbol{p}} = \sum_{\boldsymbol{k}'\boldsymbol{p}'} W_{\boldsymbol{k}\boldsymbol{p};\boldsymbol{k}'\boldsymbol{p}'}$.

We now have to work out the modified transition probability $\Pi^s_{\nu_0\nu} = \tau_\nu^s W^s_{\nu_0\nu} = \tau^s W^s_{\nu_0\nu}$. Following El-Sayed and coworkers [50], we consider a configuration ν_1 which differs from the configuration ν_0 only in the occupancy of the four momentum states $\boldsymbol{k}_1$, $\boldsymbol{p}_1$, $\boldsymbol{k}_1'$, and $\boldsymbol{p}_1'$. Then

$$\Pi^s_{\nu_0\nu_i} = P^{(1)}(\boldsymbol{k}_1, \boldsymbol{p}_1) \cdot P^{(2)}_{\boldsymbol{k}_1,\boldsymbol{p}_1}(\boldsymbol{k}_1', \boldsymbol{p}_1') \cdot P^{(3)}_{\boldsymbol{k}_1\boldsymbol{p}_1;\boldsymbol{k}_1'\boldsymbol{p}_1'}(\nu_i) \tag{8.75}$$

with

$$P^{(1)}(\boldsymbol{k}_1, \boldsymbol{p}_1) = \frac{n_{\boldsymbol{k}_1}}{N} \frac{n_{\boldsymbol{p}_1}}{N-1} \tag{8.76}$$

the probability for the electrons with momentum $\boldsymbol{k}_1$ and $\boldsymbol{p}_1$ to be the scatterer,

$$P^{(2)}_{\boldsymbol{k}_1,\boldsymbol{p}_1}(\boldsymbol{k}_1', \boldsymbol{p}_1') = \frac{W_{\boldsymbol{k}_1\boldsymbol{p}_1;\boldsymbol{k}_1'\boldsymbol{p}_1'}}{\gamma_{\boldsymbol{k}_1\boldsymbol{p}_1}} \tag{8.77}$$

the probability that the two electrons with $\boldsymbol{k}_1$ and $\boldsymbol{p}_1$ are scattered into momentum states $\boldsymbol{k}_1'$ and $\boldsymbol{p}_1'$, respectively, and

$$P^{(3)}_{\boldsymbol{k}_1\boldsymbol{p}_1;\boldsymbol{k}_1'\boldsymbol{p}_1'}(\nu_i) = \begin{cases} \frac{\gamma_{\boldsymbol{k}_1\boldsymbol{p}_1}}{\gamma}(1 - n_{\boldsymbol{k}_1'})(1 - n_{\boldsymbol{p}_1'}) & i = 1 \\ 1 - \frac{\gamma_{\boldsymbol{k}_1\boldsymbol{p}_1}}{\gamma}(1 - n_{\boldsymbol{k}_1'})(1 - n_{\boldsymbol{p}_1'}) & i = 0 \end{cases} \tag{8.78}$$

the probability for the selected momentum states to perform a real ($i = 1$) or a selfscattering ($i = 0$) event, respectively. Note, the factor $(1 - n_{\boldsymbol{k}'_1})(1 - n_{\boldsymbol{p}'_1})$ guarantees that real scattering events occur only when the final momentum states are empty. All three probabilities are normalized to unity when summed over the domain of the independent variables in the brackets.

In order to implement the ensemble-based Monte Carlo simulation, the momentum space is discretized into a large number of cells which can be either occupied or empty (see Fig. 8.7). A configuration is then specified by the occupancies of all cells. The temporal evolution of the configurations proceeds in discrete time steps τ^s and is controlled by the probability $\Pi^s_{\nu'\nu}$. The basic structure of the algorithm is thus as follows: First, the initial distribution $g_{\boldsymbol{k}}(t = 0)$ is sampled to create the initial configuration ν_0, which is then propagated in time in the following manner:

(i) Increment the time by τ^s.
(ii) Choose at random two initial momentum states, $\boldsymbol{k}_1$ and $\boldsymbol{p}_1$, and two final momentum states, $\boldsymbol{k}'_1$ and $\boldsymbol{p}'_1$.
(iii) Perform the selfscattering test consisting of two inquiries:
First, check whether the chosen momentum states are legitimate by asking whether $R_1 > P^{(1)}(\boldsymbol{k}_1, \boldsymbol{p}_1)$ and $R_2 > P^{(2)}_{\boldsymbol{k}_1,\boldsymbol{p}_1}(\boldsymbol{k}'_1, \boldsymbol{p}'_1)$, with $R_1, R_2 \in [0, 1]$ two uniformly distributed random numbers. Second, determine whether the final states are empty or not. In the former case, a real scattering event takes place provided $R_3 > P^{(3)}_{\boldsymbol{k}_1\boldsymbol{p}_1;\boldsymbol{k}'_1\boldsymbol{p}'_1}(\nu_1)$, with $R_3 \in [0, 1]$ again an uniformly distributed random variable, whereas in the latter selfscattering occurs.
(iv) Generate the new configuration ν_1, which is the old configuration ν_0 with the occupancies $n_{\boldsymbol{k}_1}$, $n_{\boldsymbol{p}_1}$, $n_{\boldsymbol{k}'_1}$, and $n_{\boldsymbol{p}'_1}$ changed in accordance to the outcome of the selfscattering test.

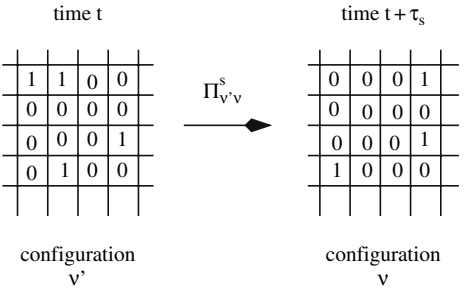

Fig. 8.7. Schematic representation of the ensemble-based Monte Carlo simulation. A sufficiently large part of the two-dimensional momentum space is discretized into small cells. Each cell with size $\Delta k_x \Delta k_y$ is labelled by its central momentum $\boldsymbol{k}_i$, $i = 1, 2, ..., M$ with M the total number of cells. An ensemble of $N < M$ electrons occupies the cells: $n(\boldsymbol{k}_i) = 1$, when an electron is in cell i, and $n(\boldsymbol{k}_i) = 0$ otherwise; $\sum_i n(\boldsymbol{k}_i) = N$. The occupancies of all cells constitute a configuration ν. During the simulation a sequence of configurations is generated stochastically whereby the transition probability from configuration ν' at time t to configuration ν at time $t + \tau_s$ is $\Pi^s_{\nu'\nu}$

The algorithm is terminated after a pre-fixed number of real scattering processes took place. The diagnostics and the calculation of moments can be done on the fly, for instance, before the time is incremented from t to $t + \tau^s$.

Provided the momentum space is appropriately discretized, the algorithm is very fast. A typical run to study, for instance, the relaxation of an initial non-equilibrium Gaussian electron distribution, $g_{\boldsymbol{k}}(t = 0) = C \exp[(E(\boldsymbol{k}) - E_0)/\sigma)^2]$, where C is a constant to fix the electron density and E_0 and σ are the position and width of the Gaussian profile, respectively, took for $N = 5000$ on the Intel 80368 processor available to El-Sayed and coworkers only 10–20 minutes [50]. With the increased computing power available now, this kind of ensemble Monte Carlo simulation is extremely fast. It should be therefore a useful tool for the simulation of dense, degenerate Fermi systems in non-equilibrium, such as, highly optically excited semiconductors, metal clusters in strong laser fields (see Chap. 9), or nuclear matter in heavy ion collisions.

8.3 Conclusions

In this section, we discussed Boltzmann transport in condensed matter, focusing on the conditions, which need to be satisfied for a BE to be applicable to the quasiparticles in a crystal, and on computational tools to solve the quasiparticle BE. Although the quasiparticle BE cannot always be rigorously derived from first principles, it provides in most cases a surprisingly accurate description of transport processes in condensed matter. Most of semiconductor device engineering, for instance, is based on a quasiparticle BE, despite the lack of a satisfying microscopic derivation.

We presented various strategies for the numerical solution of the quasiparticle BE. For the steady-state, spatially uniform, linearized BE, usually employed for the calculation of transport coefficients for metals, we discussed numerical iteration and the expansion of the one-particle distribution function in terms of a symmetry-adapted set of basis functions. In the context of condensed matter, Fermi surface harmonics are here particularly useful because they adequately describe the topology of the Fermi surface, which may be anisotropic, or even consisting of unconnected pieces in momentum space.

As far as the numerical solution of the time-dependent, nonlinear BE is concerned, we discussed iteration and Monte Carlo simulation. Both approaches have been used in the past to calculate hot electron distributions in strongly biased semiconductors. Iteration is here based on the integral representation of the BE. The approach is mathematically very elegant although its potential has not been fully exploited. By far the most popular method for the numerical solution of the BE is the Monte Carlo simulation. It has the virtue of an intuitively obvious approach, requiring a minimum of preparatory mathematical analysis, before the computer generates the solution. In addition, it requires no $\boldsymbol{k}$-summations, which makes the incorporation of realistic band structures particularly easy. We discussed two Monte Carlo algorithms. In the first, particle-based algorithm, a single test-particle is used

to build-up the stationary distribution function for electrons in a semiconductor subject to an uniform electric field. This approach, appropriately modified for time-dependent and spatially inhomogeneous settings, has become a design tool for the electronic circuit engineer, indicating its power, flexibility, and practical importance. The second approach propagates an ensemble of N electrons in discrete time steps through a discretized momentum space and is particularly useful for spatially homogeneous, degenerate electron systems with a pronounced Fermi statistics.

There are of course situations where the BE cannot be applied to condensed matter. In particular, transport properties of liquids, amorphous solids, and strongly correlated systems (transition metals, Kondo insulators etc.) cannot be described within the framework of a BE. The mean free path of quasiparticles, if they can be defined, is too short in this type of condensed matter and the separation of the quasiparticles' motion into free flights, with a few randomly occurring scattering events, is impossible. However, provided external fields and temperature gradients are weak, transport processes can be alternatively studied within linear response theory (Kubo formalism [51]). This approach relates linear transport coefficients to thermodynamic correlation functions, which can then be calculated, for instance, with the methods outlined in Chap. 19, Sect. 19.2.2. The Kubo formalism is also applicable when the mean free path is short. It is therefore the method of choice for the calculation of transport coefficients in situations where the BE cannot be used.

References

1. L.W. Boltzmann, Ber. Wien. Akad. **66**, 275 (1872) 223
2. A. Lenard, Ann. Phys. (New York) **10**, 390 (1960) 224
3. R. Balescu, Phys. Fluids **3**, 52 (1960) 224
4. G. Ecker, *Theory of fully ionized plasmas* (Academic Press, New York, 1972) 224
5. R. Winkler, in *Advances in Atomic, Molecular, and Optical Physics*, Vol. 43, ed. by B. Bederson, H. Walther (Academic Press, New York, 2000), p. 19 224, 236
6. J.M. Ziman, *Electrons and Phonons* (Oxford University Press, Oxford, 1960) 224, 229, 231, 232, 233
7. H. Smith, H.H. Jensen, *Transport Phenomena* (Clarendon Press, Oxford, 1989) 224, 229, 230, 231, 232
8. L.M. Roth, in *Handbook on Semiconductors Completely Revised Edition*, Vol. 1, ed. by P.T. Landsberg (Elsevier Science Publishers, Amsterdam, 1992), p. 489 224, 233
9. L.P. Kadanoff, G. Baym, *Quantum Statistical Mechanics* (W. A. Benjamin, Inc., New York, 1962) 224, 227
10. L.V. Keldysh, Sov. Phys. JETP **20**, 1018 (1965) 224, 227
11. E.M. Lifshitz, L.P. Pitaevskii, *Physical Kinetics* (Pergamon Press, New York, 1981) 224, 227
12. F. Bloch, Zeitschrift f. Physik **52**, 555 (1928) 224
13. R. Peierls, Ann. d. Physik **3**, 1055 (1929) 224
14. L.D. Landau, Sov. Phys. JETP **3**, 920 (1958) 224
15. R.E. Prange, L.P. Kadanoff, Phys. Rev. **134A**, 566 (1964) 227
16. G. Eilenberger, Zeitschrift f. Physik **214**, 195 (1968) 227
17. A.I. Larkin, Y.N. Ovchinnikov, Sov. Phys. JETP **28**, 1200 (1969) 227
18. G. Eliashberg, Sov. Phys. JETP **34**, 668 (1972) 227
19. A.I. Larkin, Y.N. Ovchinnikov, Sov. Phys. JETP **41**, 960 (1976) 227

20. D. Rainer, in *Recent Progress in Many-Body Theories*, Vol. 4, ed. by E. Schachinger, H. Mitter, H. Sormann (Plenum Press, New York and London, 1995), p. 9 227
21. D. Rainer, Prog. Low Temp. Phys. **10**, 371 (1986) 227
22. B. Nicklaus, *Quasi-particle picture and ab-initio band structure of electrons in solids: Transport and superconducting properties (in German)* (PhD Thesis, Universität Bayreuth, 1993) 227
23. V. Špička, P. Lipavský, Phys. Rev. B **52**, 14615 (1995) 227
24. I.M. Lifshitz, M.I. Kaganov, Sov. Phys. Usp. **2**, 831 (1960) 228
25. H.H. Jensen, H. Smith, J.W. Wilkins, Phys. Lett. **27B**, 532 (1968) 230
26. J. Sykes, G.A. Brooker, Ann. Phys. **56**, 1 (1970) 230
27. K. Takegahara, S. Wang, J. Phys. F: Metal Phys. **7**, L293 (1977) 231, 233
28. C.R. Leavens, J. Phys. F: Metal Phys. **7**, 163 (1977) 231, 233
29. H.L. Engquist, Phys. Rev. B **21**, 2067 (1980) 231, 233
30. H.L. Engquist, G. Grimvall, Phys. Rev. B **21**, 2072 (1980) 231, 233
31. H. Budd, Phys. Rev. **158**, 798 (1967) 231, 233, 234
32. H.D. Rees, J. Phys. Chem. Solids **30**, 643 (1969) 231, 233, 235
33. M.O. Vassel, J. Math. Phys. **11**, 408 (1970) 231, 233, 235
34. H.D. Rees, J. Phys. C: Solid State Phys. **5**, 641 (1972) 231, 233, 235
35. C. Hammar, J. Phys. C: Solid State Phys. **6**, 70 (1973) 231, 233, 236
36. P.B. Allen, Phys. Rev. B **13**, 1416 (1976) 231, 237
37. P.B. Allen, Phys. Rev. B **17**, 3725 (1978) 231, 236, 237, 238, 239
38. F.J. Pinski, Phys. Rev. B **21**, 4380 (1980) 231, 236, 238, 239
39. F.J. Pinski, P.B. Allen, W.H. Butler, Phys. Rev. B **23**, 5080 (1981) 231, 236, 239
40. T.P. Beaulac, P.B. Allen, F.J. Pinski, Phys. Rev. B **26**, 1549 (1982) 231, 236, 239
41. I. Mertig, E. Mrosan, J. Phys. F: Metal Phys. **12**, 3031 (1982) 231, 236, 239
42. T. Vojta, I. Mertig, R. Zeller, Phys. Rev. B **46**, 15761 (1992) 231, 236, 239
43. W.W. Schulz, P.B. Allen, Phys. Rev. B **52**, 7994 (1995) 231, 236, 239
44. W. Fawcett, A.D. Boardman, S. Swain, J. Phys. Chem. Solids **31**, 1963 (1970) 231, 240, 244
45. C. Jacoboni, L. Reggiani, Rev. Mod. Phys. **55**, 645 (1983) 231, 234, 240
46. M.V. Fischetti, S.E. Laux, Phys. Rev. B **38**, 9721 (1988) 231, 240, 247
47. C. Jacoboni, P. Lugli, *The Monte Carlo Method for Semiconductor Device Simulation* (Springer-Verlag, Wien, 1989) 231, 240, 247
48. C. Moglestue, Rep. Prog. Phys. **53**, 1333 (1990) 231, 240, 247
49. M.V. Fischetti, S.E. Laux, P.M. Solomon, A. Kumar, J. Comp. Electr. **3**, 287 (2004) 231, 240, 247
50. K. El-Sayed, T. Wicht, H. Haug, L. Bányai, Z. Phys. B **86**, 345 (1992) 231, 248, 250, 252
51. R. Kubo, J. Phys. Soc. Japan **12**, 570 (1957) 253